CHAPTER 12 MOVEMENT OF TROPICAL CYCLONES ^

^ *Chapter 12 was edited by Prof. Johnny Chan*

CHAPTER 12 - MOVEMENT OF TROPICAL CYCLONES

12.1 Introduction

As early as 1841, Espy (1841) hypothesized that tropical cyclones were carried along in the prevailing larger-scale atmospheric flow in which they were embedded rather like eddies in a river. This concept is known as "steering". It has received support since the days when it was first possible to prepare charts of monthly mean surface pressure and determine cyclone tracks with reasonable accuracy, for it could then be seen that the tracks often tended to parallel the mean surface isobars. Indeed, the well known near parabolic shape of many typhoon tracks would be expected if typhoons moved with the flow around the periphery of the Pacific anticyclone. This phenomenon is illustrated by the four tracks in September 1959, shown in Fig. 12.1, superimposed upon a chart of the average surface pressure for that month; the fit is not perfect of course; the pressure pattern for each day is not identical to the mean for the whole month.

The first problem in applying the steering concept to individual cases is that the broad-scale steering flow is not always readily apparent. In most cases the storm itself largely obscures the basic current in the area of interest. It is necessary therefore to subtract the wind (or pressure) field due to the storm from the prevailing field. Unfortunately, this cannot be done quantitatively without assuming the form of the storm wind (or pressure) field. Even if the latter could be specified, it is known that tropical cyclones affect the environment beyond their outermost closed isobar.

A second problem in applying the steering concept arose when it was found that tropical cyclones did not always move with what appeared to

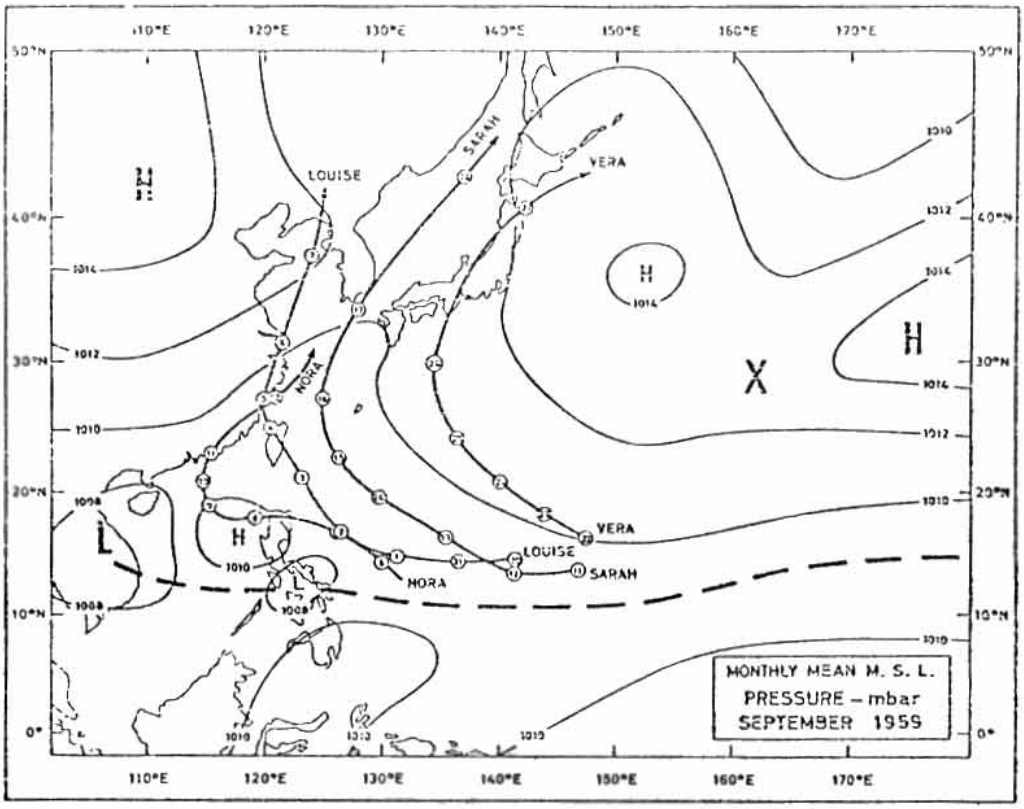

Fig. 12.1. The tracks of four typhoons which formed in September 1959 shown here together with mean surface pressure for the month. The typhoons moved around the Pacific ridge along classic, near parabolic tracks. X marks the centre of the Pacific anticyclone at 700 mbar. The dashed line marks the mean location of the equatorial trough.

be well-defined broad-scale flows at the surface. A typical example is shown in Fig. 12.2 (a). To meet these occasions, it was hypothesized that the storm was "steered" by the flow at some higher level as illustrated in Fig. 12.2(b). When charts showing the upper wind flow became available, a level could usually be found - after the event - at which the generalized flow in the area of a cyclone had a speed and direction which agreed with the movement of storm - this level became known as the "steering level". A long controversy then began amongst meteorologists as to exactly which level was the steering level. Over the years every standard level from the surface to 200 mbar has at some time been advocated as the steering level. Some meteorologists have, for a number of years, maintained that the level at which the storm circulation disappeared from working charts - usually 300 mbar or 200 mbar - is the steering level. At this level, they reasoned, the steering flow was not obscured by the storm circulation. More than 30 years after the widespread introduction of upper-air soundings and charts, some meteorologists were still advocating a particular level at which - they maintain - the basic currents determine the movement of tropical cyclones. Post-analysis reports on the tracks of tropical cyclones still include statements to the effect that "the storm was steered by the flow at such and such a level". Over the years, the hypothesis that there is such a steering level has not easily been confirmed or disapproved due to the problem of the masking of the basic current by the storm circulation. Also, the number of observations at upper levels has usually been inadequate to decide the matter.

The steering concept is easily applied to explain tropical cyclone movement if the currents at all levels in the troposphere are well

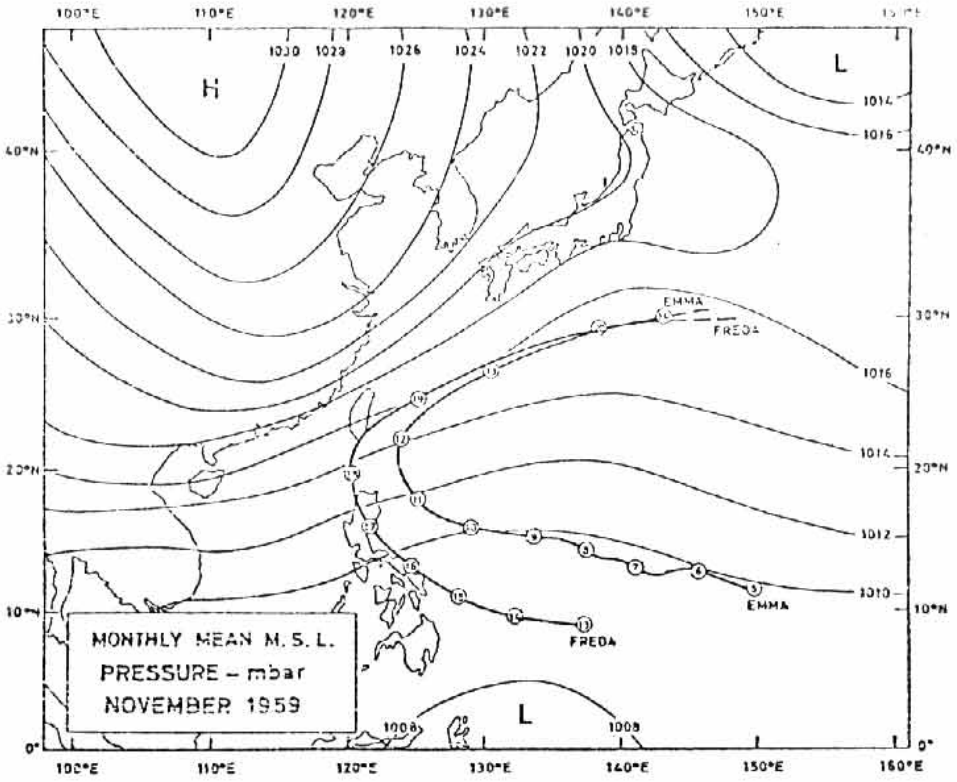

(a)

Fig. 12.2 a–b. The tracks of typhoons Emma and Freda in November 1959 are here shown superimposed on charts of (a) the mean surface pressure and (b) the contours of the 700 mbar surface for the same month. The two tracks tend to parallel the mean contours at 700 mbar whereas they show little relationship with the flow at the surface as indicated by the mean isobars.

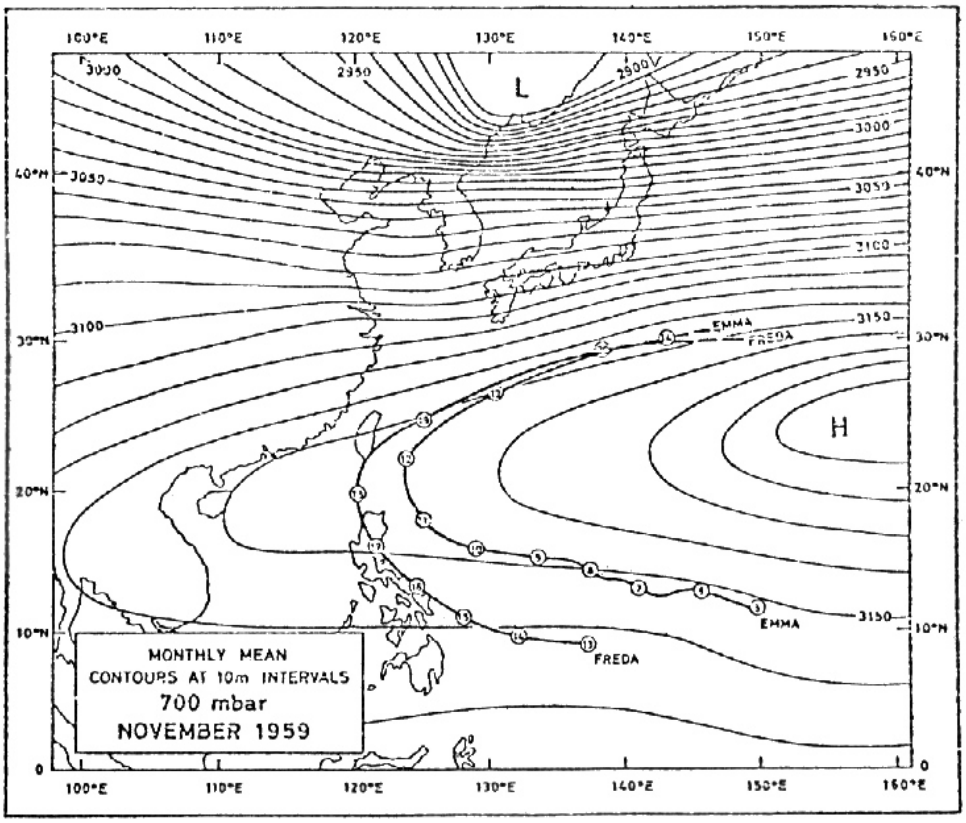

(b)

Fig. 12.2 a-b. Continued.

defined and similar for then, they all indicate the same movement and the choice of level is not important. Difficulties arise in the much more frequent cases when the currents at different levels, if they can be reliably determined, give different indications. The level that gives the best indication on one occasion may not do so on the next. The problem is therefore not simple. The basic currents in the whole troposphere around a storm affect its motion and there is also a dynamic component of motion due to the interaction between the storm and its environment - which it helps shape.

In addition to the problem of determining the basic current carrying the storm along and the interaction effects, there are reasons for believing that there are internal forces within a tropical cyclone which also affect its motion. A proper understanding of the problem must therefore consider firstly the integrated influence of the environment throughout the depth of the storm, and secondly, the contribution of any internal forces. To be able to forecast the movement of tropical cyclones - the subject of this chapter - it is necessary to go further and consider future changes in the environmental flow due to large-scale, global adjustments and also regional contributions to these changes attributable to the storm itself.

12.2 Steering Flow

As discussed in the introduction, tropical meteorologists have tried over the last few decades to determine the steering flow and the steering level. Basically, two methods have been used. The first one determines a geostrophic current from a height or pressure gradient across the cyclone. The geostrophic flows at different levels are then compared with the cyclone motion vector. The flow that most closely approximates the latter is assumed to be the steering flow and the level at which this flow is situated is called the steering level.

The other method tries to locate an actual wind vector at some distance away from the cyclone center that matches the cyclone motion vector. An alternative version of this technique relates the azimuthally-averaged flow around the cyclone to the cyclone motion vector. This latter method has the advantage of filtering out much of the asymmetry in the observed flow so that a "mean" current may be determined.

Different researchers used different samples of tropical cyclones in their studies. In most cases, such samples are rather limited in the number of cases and the types of cyclones included. Thus, a diversity of conclusions have been arrived, as illustrated in Table 12.1. Individual levels or combinations of them from the surface to 200 mb have been determined as the steering level. A good review of these studies can be found in George (1975). Some operational versions of these studies are also discussed in a World Meteorological Organization report (WMO, 1979). The reader is referred to these two publications for further discussion of individual techniques.

TABLE 12.1

Examples of previous researh to define steering level(s) for tropical cyclone motion (adapted from George, 1975).

Author(s)/Year	Primary Levels Used for Steering
Riehl and Shafer (1944)	700,500 mb
Simpson (1946)	Top of vortical circ.
Riehl and Burgner (1950)	Sfc. to 300 mb
Gentry (1951)	Top of vortical circ.
E. Jordan (1952)	Sfc. to 300 mb
Riehl *et al*. (1956)	500 mb
Miller and Moore (1960)	700, 500, 300 mb
Sanders and Burpee (1968)	Sfc. - 100 mb
Renard (1968)	700 mb
Chin (1970)	700, 500 mb

In most of the steering flow studies, effort has been concentrated on matching the cyclone motion vector and some atmospheric flow vector (actual observed wind or geostrophic wind). Recently, some studies have been performed to document further the relationship between the steering flow and tropical cyclone motion. These studies are partly a result of an apparent discrepancy between observational and numerical studies. For example, Jones (1977) found that his model vortex moved at an angle of 5^{o} to the <u>right</u> of the steering current which is uniform easterly flow of 10 m s^{-1}. Despite differences in their model characteristics (spatial resolution, numerical and physical parameterization techniques, etc), Madale and Piacsek (1975), Anthes and Hoke (1975) and Chang and Madala (1980) all reported that the vortex in their numerical models moves to the <u>right</u> of the steering current which, in most cases, is similar to that defined by Jones (1977). In earlier theoretical studies by Yeh (1950) and Kuo (1969), the model vortex was also found to have a mean path that is biased to the right of the superimposed current. Such a deviation between the cyclone motion vector and the model-imposed flow has been attributed to the surface drag or the Rossby effect (Rossby, 1948). These "internal forces" will be discussed further in the next section.

Observational studies, on the other hand, suggest that tropical cyclones in the Northern Hemisphere in general have a tendency to move to the <u>left</u> of the mean steering current. George and Gray (1976) and Gray (1977) performed comprehensive rawinsonde composite studies of tropical cyclones in the northwest Pacific and the west Atlantic respectively. Their samples consist of cyclones with widely different characteristics (direction, speed, intensity, intensity change, etc).

They defined their steering current as the azimuthally-averaged flow within the 1^{o}–7^{o} latitude radial band around the tropical cyclone. They found that their composite cyclones move at an angle of ~ 10^{o}–20^{o} to the left of this steering current in the mid-troposphere (500-700 mb). Brand, et al. (1981) used the 500 mb geostrophic wind surrounding a tropical cyclone as the steering current. They found that on the average, cyclones move at an angle of 6^{o} to the left of the average geostrophic flow. However, variations exist within their sample, with cyclones in the lower latitudes move less to the left and sometimes even to the right of the steering current. As the latitude of the cyclone increases, so does the amount of leftward deviation of the cyclone motion vector from the mean geostrophic flow. Recently, Chan and Gray (1982) re-analyzed and expanded the data sets of George and Gray (1976) and Gray (1977). They also included in their study for the first time, tropical cyclones in the Southern Hemisphere. With the steering current defined as the azimuthally-averaged flow only within the 5–7^{o} latitude radial band, they found that in general, the composite cyclones in the Northern Hemisphere move at ~ 10^{o}–20^{o} to the left of this steering current in the mid-troposphere while those in the Southern Hemisphere move to the right of the steering current by approximately the same amount. However, cyclones with a significant zonal component of motion appear to move differently from the mean case, with westward-moving cyclones in the Northern Hemisphere moving less to the left or even to the right of the steering flow. An opposite relation holds for westward-moving cyclones in the Southern Hemisphere. In an extensive study of tropical cyclones in the Southern Hemisphere, Holland (1983) drew similar conclusions.

This apparent discrepancy between observations and results of numerical studies seems to be related to the "interval forces" that affect the path of a tropical cyclone. These forces and their dynamics will be discussed in the next section. As of now, it suffices to say that the results of these basic studies (observational, theoretical and numerical) of the relationship between tropical cyclone motion and its surrounding flow together with those of other steering flow studies all point to the fact that the surrounding flow, as important as it may seem to be, is <u>not</u> the only determining factor in tropical cyclone motion. Other dynamical processes exist to modify the motion vector defined by the large-scale flow. Therefore, the steering flow concept can only be considered as approximately valid. Forecasters in the field must bear in mind those research results and modify their track predictions accordingly.

12.3 Internal Forces

12.3.1 Meridional Motion

The great majority of tropical cyclones move poleward throughout their life even at times when no external steering current is discernable. Furthermore, as discussed in the last section, the motion of a cyclone centre usually shows departures from the apparent steering flow. Some internal forces which might account for these effects have been identified.

Rossby (1949) found that there should be a net force on an axisymmetric vortex. The force, due to the variation of the Coriolis parameter with latitude (the beta-effect) across the vortex, is in a direction which would cause cyclones to drift polewards and anticyclones equatorwards. This phenomenon, known as the "Rossby effect", comes about as the result of imbalance between the velocity and mass fields. For a normal flow around a low-pressure center with a given curvature and spacing of isobars, the gradient wind increases with decreasing latitude. Therefore, the equatorward side of a symmetrical tropical cyclone would transport more air eastward than is carried westward on the poleward side. Air is thereby depleted from the westward half of the cyclone and accumulated in the eastern half. If this pattern is maintained throughout the troposphere, the surface pressure will fall in the west of the storm and rise in the east. The resulting pressure gradient across the cyclone would, according to Rossby, cause it to accelerate poleward although Bjerknes and Holmboe (1944) suggested that a westward movement would result. The phenomenon can also be interpreted as the conversion of the earth's vorticity into cyclonic relative vorticity to the west of a storm centre and into anticyclonic

relative vorticity to the east, the resulting northward current through the typhoon causing the northward motion (Jones 1977c Anthes, 1982). Adem (1956) found that the beta-effect would cause a symmetric, non-divergent vortex to first accelerate westward but soon turn northward.

The effects described above should be greatest in low latitudes where the change of the Coriolis parameter with latitude is most rapid. Riehl (1954) also pointed out that large typhoons should drift northward faster than small ones because of the greater change in Coriolis parameter across these larger storms. More specifically, Dunn and Miller (1960) stated that a large storm should drift northward at 1^{o} to 3^{o} latitude per day but that for very small storms the drift is almost negligible.

Cressman (1951) applied the Rossby principle to typhoons and deduced that the northward acceleration should depend on the radial velocity profile and the extent of the typhoon. Cressman's calculations indicated an insignificant poleward acceleration for a small but intense typhoon increasing to about 9 m s^{-1} per day for Doris 1950, a large mature typhoon with radius 1 100 km and a maximum wind speed of 62 m s^{-1}. However, Gentry (1952) considered that the acceleration, if any, should be much less than that indicated by Cressman's calculation on surface winds. Gentry maintained that, among other things, the calculation should be extended through all layers to the top of the typhoon and that the contribution from the upper levels, where the circulation is anticyclonic, would be in a direction opposite to that from low levels. Petersen (1950) from a more general argument showed that the meridional motion of a cyclone centre due to the beta-effect depends on whether there is convergence or divergence near the centre. In a typhoon with

low-level convergence and high level divergence the resultant force should be small and change little throughout the life of the storm. In addition, Long (1951) has shown that there is a net pressure force acting on a vortex which is very nearly equal to one-half the resultant of the Rossby force, and is oppositely directed.

Numerical modelling of tropical cyclones in an extended environment has not yet advanced to a stage where the internal forces can be reliably determined. Anthes and Hoke (1975) found a 1.4 to 2.8 m s^{-1} northerly drift in their two models. Jones (1977c) found northerly acceleration in agreement with Rossby's theory for only 24 hours, thereafter the acceleration decreased and a quasi equilibrium was attained at 36 hours. Rosenthal (1976) found that the mechanics by which the beta-effect produces accelerations in the movement of vortices lay primarily in differential advection of absolute vorticity between the east and west sides of an initially symmetric vortex as discussed by Adem (1956). However, since real tropical cyclones are asymmetric he concluded that accelerations due to differential vorticity advection could be in any direction depending on the instantaneous distribution of vorticity asymmetries. In two similar analytical studies, Chan (1982) and Holland (1983) found that the meridional motion of a symmetric vortex in a uniform current depends on the divergence associated with the vortex. Chan further showed that when the surrounding flow is not uniform (sheared or divergent), the meridional motion of the vortex varies according to the dynamic characteristics of this flow.

The diversity of the results of numerical and theoretical studies of internal forces illustrates the intractable nature of the problem. Some information on these forces can be obtained by examining the actual

movement of typhoons and other systems. However, this direct approach also has limitations in so far as the precise contribution to storm movement due to steering or interaction with environmental flow is almost always unknown. In a general study of the 24-hour movement of cyclones and anticyclones on Northern Hemisphere weather charts over a two-year period and seven latitude bands, Macdonald (1967) found that the preferred motion of anticyclones was eastwards and southwards at all latitudes; cyclones moved northwards and eastwards on average except that, in the tropics, the average zonal motion was towards the west. Outside the tropics, the described movement of vortices is partly due to the fact that cyclones are most frequently under the southwesterly winds downstream from mid-tropospheric troughs while anticylones are influenced by the northwesterly currents in the rear. The correlation between the meridional motion of cyclones and their size was negative between 30° and 40°N and zero between 10° and 30°. Ramage (1961) in a more specialized study analyzed the median poleward movement of typhoons of different sizes for the period 1899-1938. He also found that there was no significant connection between circulation size and northward movement and concluded that, if there was such an effect due to variation of the Coriolis parameter, then it was well hidden.

An analysis of the poleward movement of a large number of tropical storms and typhoons which were well observed by aircraft reconnaissance and other methods during the period 1958-1974 is shown in Table 12.2. (Statistical details have been included in this table to show the general run of sample sizes and the spread in the observations, these details will be omitted from the next two tables.) The overall average poleward movement is shown as 1.9° latitude per day (2.4 m s^{-1}). The

TABLE 12.1

Subsequent 24-Hour Poleward Movement Of Tropical Storms And Typhoons Of Different Sizes In Different Latitude Bands (Period 1958 - 1974)

Latitude of Centre		Radius of outer isobar in degrees latitude*				
		0.0-1.4	1.5-2.9	3.0-4.4	Above 4.4	All sizes
°N		degrees latitude				
0.0-9.9	Median	0.9	1.0	1.5	1.3	1.3
	Mean	1.1	1.0	1.6	1.4	1.3
	Std. Dev.	1.0	1.0	1.0	1.0	1.0
	No. of Cases	23	123	113	93	352
	Maximum	3.3	3.6	4.3	5.8	5.8
10.0-19.9	Median	1.6	1.6	1.6	1.8	1.7
	Mean	1.4	1.7	1.6	1.9	1.7
	Std. Dev	1.6	1.5	1.6	1.4	1.5
	No. of Cases	89	766	872	824	2551
	Maximum	6.3	8.3	8.7	8.4	8.7
20.0-29.9	Median	2.1	2.4	2.3	2.3	2.3
	Mean	2.5	2.5	2.3	2.6	2.5
	Std. Dev.	2.6	2.2	1.9	2.2	2.1
	No. of Cases	37	368	455	523	1383
	Maximum	9.4	12.9	9.8	11.7	12.9
30.0 and above	Mediam	-0.3	2.3	1.9	2.1	2.1
	Mean	0.4	2.7	1.6	2.5	2.2
	Std. Dev.	1.5	2.5	1.9	2.6	2.4
	No. of Cases	3	50	46	29	128
	Maximum	2.1	10.2	6.9	9.3	10.2
All latitudes	Median	1.5	1.8	1.7	1.9	1.8
	Mean	1.6	1.9	1.8	2.1	1.9
	Std. Dev.	1.9	1.8	1.7	1.8	1.8
	No. of Cases	152	1307	1486	1469	4414
	Maximum	9.4	12.9	9.8	11.7	12.9

*Isobars are drawn at 2 mbar intervals.

movement increases with latitude from 1.3° per day (1.7 m s^{-1}) south of 10°N to 2.5° per day (3.2 m s^{-1}) between 20°N and 29.9°N. South of 20°N large storms move poleward, on average, about 30% faster than small ones. Although the size of typhoons has a statistically significant influence on their poleward movement south of 30°N (Table 12.5) the magnitude of the movement is controlled primarily by the environment. This is shown in Table 12.3 where the poleward acceleration of storms in terms of latitude and size is given. The acceleration was obtained by subtracting the poleward movement over the 24 hours prior to an aircraft fix from that over the subsequent 24 hours. In this way the steady effect of steering and interaction is eliminated and the accelerations can be attributed to internal forces and changes in external steering if any. The correlation between storm size and poleward acceleration is shown in Table 12.5 and is highly significant in all latitude bands. South of 20°N the average poleward acceleration of large storms (Table 12.3) is more than twice that of small ones. The effect of latitude is seen insofar as storms of all sizes south of 10°N accelerate at least twice as fast, on average, as those between 10°N and 19.9°N. The acceleration also increases in the 20°N to 29.9°N band. North of 30°N large storms maintain their poleward acceleration while small ones decelerate. Storms frequently recurve north of 20°N and the environmental influences there will then be changing and so affect the accelerations.

The Rossby effect is not determined only by vortex latitude and size but is also dependent on vortex intensity. Accordingly, deep typhoons should, on average, accelerate polewards more rapidly than weaker ones and, amongst those of the same intensity, the storms in

TABLE 12.2

Subsequent 24-hour average movement and acceleration of tropical storms and typhoons by size in different latitude bands.

Radius of outer isobar in degrees latitude*

Latitude of centre in degrees north	0.0–1.4	1.5–2.9	3.0–4.4	>4.4	All sizes	0.0–1.4	1.5–2.9	3.0–4.4	> 4.4	All sizes
	Poleward movement °lat/24h					Eastward movement °lat/24h				
0.0–9.9	1.1	1.1	1.6	1.4	1.3	-3.4	-3.6	-4.1	-3.3	-3.7
10.0–19.9	1.4	1.7	1.6	1.9	1.7	-2.5	-2.8	-2.7	-2.9	-2.8
20.0–29.9	2.5	2.5	2.3	2.6	2.5	-1.7	-1.1	-0.5	-0.3	-0.6
≥30.0	---	2.7	1.6	2.5	2.2	---	1.1	2.6	3.1	2.2
All latitudes	1.6	1.9	1.8	2.1	1.9	-2.3	-2.3	-2.0	-1.9	-2.0
	Poleward acceleration °lat/24h/24h					Eastward acceleration °lat/24h/24h				
0.0–9.9	---	0.5	0.7	1.0	0.6	---	-0.3	-0.2	-0.8	-0.4
10.0–19.9	---	0.2	0.2	0.5	0.3	0.2	0.6	0.5	0.3	0.4
20.0–29.9	0.5	0.3	0.4	0.7	0.5	0.9	0.8	0.9	1.0	0.9
≥30.0	---	-0.3	-0.8	0.9	-0.2	---	2.1	1.1	1.3	1.6
All latitudes	0.0	0.3	0.3	0.6	0.4	0.5	0.6	0.6	0.6	0.6

A dash indicates that the sample size N is less than 20.

* Isobars are drawn at 2 mbar intervals.

lower latitudes should accelerate the fastest. Although Table 12.4 shows clearly that the average poleward movement is dependent on intensity, with deep typhoons moving poleward about twice as fast as weak ones. However, the poleward acceleration does not appear to be so dependent. The correlation between typhoon intensity and poleward movement is shown in Table 12.5 to be highly significant whereas the poleward acceleration, south of 30°N, is not significantly correlated with intensity. These features are brought out most clearly if only storms with pressures of 980 mbar or less are considered, as in Table 12.5. If storms of all intensities are correlated with poleward acceleration an overall significance level of 1% is obtained but in the individual latitude bands significant results are obtained only between 10°N and 20°N and north of 30°N. The fact that the poleward movement of typhoons is highly correlated with their intensity whereas the poleward acceleration is not so correlated indicates firstly, that in nature the contribution of intensity to the Rossby effect is minimal and secondly, that the deeper the typhoon the more likely it is to be found in an environment with a strong poleward component of motion.

The observations in Table 12.4 also show the poleward acceleration of typhoons south of 10°N to be greater than those of the same intensity between 10°N and 19.9°N. The greater average poleward acceleration shown in all intensity ranges for the latitude band 20°N to 29.9°N is probably a consequence of the interaction with the environment because it is here that typhoons most frequently attain their greatest intensity and simultaneously come under the influence of the westerlies and begin recurvature.

TABLE 12.3

Subsequent 24-hour average movement and acceleration of tropical storms and typhoon by intensity in different latitude bands

Central minimum pressure in mbar

Latitude of centre in degrees north	<910	910 to 929	930 to 949	950 to 969	970 to 989	>989	All pressures	<910	910 to 929	930 to 949	950 to 969	970 to 989	>989	All pressures
	Poleward movements °lat/24h							Eastward movements °lat/24h						
0.0–9.9	---	---	---	1.3	1.3	1.4	1.4	---	---	-3.3	-4.3	-4.0	-3.3	-3.7
10.0–19.9	2.4	2.2	2.1	1.9	1.6	1.4	1.7	-3.7	-2.7	-2.3	-2.5	-2.8	-2.8	-2.7
20.0–29.9	4.0	3.0	3.0	2.5	2.3	1.9	2.5	-1.4	-1.5	-0.3	-0.5	-0.7	-1.0	-0.7
≥30.0	---	---	---	2.5	1.3	0.3	2.1	---	---	---	2.5	1.7	0.0	2.0
All latitudes	2.8	2.5	2.6	2.2	1.8	1.4	1.9	-3.2	-2.1	-1.3	-1.3	-2.1	-2.7	-2.0
	Poleward acceleration °lat/24h/24h							Eastward acceleration °lat/24h/24h						
0.0–9.9	---	---	---	0.6	0.8	0.5	0.7	---	---	---	0.3	-0.5	-0.6	-0.4
10.0–19.9	0.3	0.3	0.5	0.4	0.3	0.1	0.3	0.5	0.6	0.9	0.4	0.3	0.2	0.4
20.0–29.9	0.8	0.6	0.7	0.5	0.5	0.3	0.5	1.4	0.8	1.6	0.7	0.5	1.0	0.9
≥30	---	---	---	-0.2	-0.8	---	-0.3	---	---	---	1.5	1.2	---	1.4
All latitudes	0.5	0.4	0.7	0.4	0.3	0.2	0.4	0.7	0.7	1.3	0.6	0.3	0.2	0.6

dash indicates that the sample size N is less than 20.

TABLE 12.4

Correlation coefficients (r) and their significance (sig.) for the relationships between the 24-hour movement and acceleration of typhoons and their size and intensity. Number of pairs N.

		MOVEMENT						ACCELERATION					
	Latitude of centre	Poleward			Eastward			Poleward			Eastward		
	°N	r	N	sig.	r	N	sig.	r	N	sig.	r	N	sig.
	0–9.9	0.13	352	2%	0.042	352	n.s.	0.18	197	1%	-0.24	197	<0.1%
	10–19.9	0.078	2552	<0.1%	-0.019	2552	n.s.	0.098	1889	<0.1%	-0.065	1889	1%
STORM	20–29.9	0.053	1383	5%	0.12	1383	<0.1%	0.13	1229	<0.1%	0.063	1229	5%
RADIUS	≥30	0.017	128	n.s.	0.19	128	5%	0.23	119	1%	-0.15	119	n.s.
	All lat.	0.079	4415	<0.1%	0.054	4415	<0.1%	0.12	3434	<0.1%	-0.010	3434	n.s.
	0–9.9	-0.31	80	1%	-0.30	80	1%	-0.029	65	n.s.	-0.25	65	5%
	10–19.9	-0.14	993	<0.1%	0.047	993	n.s.	0.022	915	n.s.	-0.066	915	5%
STORM	20–29.9	-0.16	893	<0.1%	0.037	893	n.s.	-0.047	863	n.s.	-0.12	863	<0.1%
INTENSITY[+]	≥30	-0.40	93	<0.1%	0.029	93	n.s.	-0.28	90	1%	-0.21	90	5%
	All lat.	-0.15	2059	<0.1%	0.056	2059	2%	-0.028	1933	n.s.	-0.083	1933	<0.1%

[+] Storm central pressure less than or equal to 980 mbar.

The poleward steering of tropical cyclones has been related to the east and west gradient of the height of a pressure surface across them. Riehl, et al. (1956) used the 500 mbar surface, Miller and Moore (1960) and Tse (1966) used that at 700 mb. Their equations for the meridional motion when there is no height difference across a storm - assumed equivalent to no steering - yield residual motions over 24 hours of 0.8°, 1.5° and 0° respectively. Other similar experiments have yield results within this range. Unfortunately, these estimates are also affected by steering because it is known (Viegas Miller 1958, Tse 1966, George 1975) that storm motion responds to conditions beyond the 10° - 15° radii considered when measuring the gradients of height (see Fig. 12.11).

From the foregoing discussion it is clear that although typhoons move poleward on average in all latitudes, and although this movement is strongly and positively correlated with the intensity and latitude of the storms and less strongly correlated (south of 30°N) with storm size, it is not yet clear how much of this motion is to be attributed to internal forces and how much to the environmental flow and interaction. Any poleward acceleration which may be caused by internal forces seems, on average and south of 30°N, to be positively correlated with storm size but uncorrelated with storm intensity. Numerical models, insofar as they can currently approximate real conditions, point to the importance of circulation asymmetries as a cause of internal forces. Although asymmetries in the typhoon inflow can often be identified the outflow in the upper troposphere normally exhibits gross asymmetry which may well be a dominant factor in determining the poleward acceleration of tropical cyclones as suggested by Riehl (1956).

12.3.2 Zonal Motion

Although there may still be doubt about the contributions of systematic internal forces driving typhoons poleward the evidence for any such systematic forces causing zonal motion is even less substantial. Insofar as he can identify a situation in which a typhoon is isolated from its environment, an experienced meteorologist expects a slow northerly drift but, he would not normally expect a zonal component of motion in such cases. Zonal motion can of course, be caused by storm asymmetry as discussed in the previous section. Bjerknes and Holmboe (1944) considered that the beta-effect should cause axisymmetric cyclones to move towards the west but this result is not directly applicable to typhoons because the anticyclonic outflow in their upper levels would tend to give rise to an opposing easterly force.

When a vortex is moving in a steering current Rossby (1949) and Adem (1956) argued that the beta-effect should cause the absolute magnitude of the zonal motion of the vortex to be inversely proportional to its horizontal dimensions. Kasahara (1957, 1959) has also shown that the absolute magnitude of zonal motion should be less for large vortices and that under certain restrictive conditions and, in particular, ignoring any relative vorticity due to the steering current, the zonal component of motion of the vortex centre C_x is given by

$$C_x = u - L^2\beta/4 \qquad (12.1)$$

where u is the zonal component of the steering current in m s^{-1}, L the radial distance in metres from the vortex centre to a point where the vorticity vanishes and β is the gradient of the Coriolis parameter. In typhoons L can range from 100 to 1000 km and at $15^{o}N$, $\beta = 2.21 \times 10^{-11}$ rad m^{-1} s^{-1} so that the retardation - second term - could range from 5.5

m s^{-1} for a large typhoon to 0.05 m s^{-1} for a small one. In a steering current of 5 m s^{-1} a large storm could therefore be expected to remain stationary.

The average observed zonal movement of typhoons and tropical storms in 24 hours is shown in Table 12.3. The westerly movement of 3.7° per day (4.8 m s^{-1}) south of 10°N decreases northward to 0.6° per day (0.8 m s^{-1}) between 20°N and 29.9°N. North of 30°N the average motion is towards the east at 2.2° per day (2.8 m s^{-1}). Table 12.5 shows that, as found by Macdonald (1967), the zonal motion of storms in low latitudes (<20°N) is not correlated with their size. Between 20°N and 29.9°N the average westerly displacement is highly correlated with storm size being less for larger storms. However, north of 30°N the eastward movement increases with typhoon size at a level of significance of 5%. This result is contrary to the findings of Macdonald (1967) for cyclones in general and is not in agreement with Eq. (12.1). Large storms north of 30°N will more easily draw in colder air and take on extratropical characteristics than will small ones. This may affect their zonal displacement. The movement of 29 large typhoons north of 30°N was examined; 17 were shown on the Japanese-published weather charts as becoming extratropical. Of these 17, twelve moved eastward faster than 3.1° per day whereas only one of the non-frontal tropical storms exceeded this speed. This result is statistically significant and consistent with the hypothesis that north of 30°N tropical storms which take on extratropical characteristics travel faster than those which do not change their character. However, the subject needs more detailed study.

South of 10°N the average zonal acceleration is towards the west

(Table 12.3) probably because most storms acquire a more easterly environment as they develop by both drifting poleward and developing vertically. North of 10°N the average acceleration is eastward as the developed storms move out of the easterlies and towards westerlies. South of 20°N the average eastward acceleration is negatively correlated with typhoon size, the correlation being highly significant to the south of 10°N (Table 12.5).

There is no significant variation of zonal movement with storm intensity except that south of 10°N deep storms tend to move westward faster than weak ones (Table 12.5) probably for reasons given in the previous paragraph. However, the zonal acceleration of typhoons towards the east has a significant negative correlation with storm intensity in all latitudes (Table 12.5). This means that, on average, deeper storms are accelerated more towards the east than weaker ones. Again, this effect is not necessarily due to internal forces but is more probably due to synoptic features favorable for deepening typhoons being also associated with increased steering towards the east.

When the north to south gradient of height across a tropical cyclone is zero the residual zonal motion indicated by the forecast techniques of Riehl *et al.* (1958) and Tse (1966) - mentioned in the previous section - is zero. The technique of Miller and Moore (1960) indicates a residual 24-hour movement of 0.92° towards the west. However, for reasons stated earlier this figure must be taken with reservations.

In summary, typhoons and tropical storms, on average, have a component of motion towards the west which decreases with latitude until, above 30°N, it becomes easterly. In general, the zonal movement

is dependent on storm size northward of 20°N where large storms move faster towards the east and on storm intensity to the south of 10°N where deep storms move slower towards the west (Table 12.5). On average, the more intense a storm the greater is the acceleration towards the east at all latitudes. South of 20°N large storms tend to have less eastward acceleration than small ones. There is little evidence that isolated typhoons experience any internal force such as would, on average, cause them to move in an east or west direction.

12.3.3 Oscillatory Motion

Lamb (1932) showed that the two dimensional motion of a rotating cylinder in a rotating fluid would, under certain conditions, be represented by a trochoidal path in a general direction parallel to the stream. From a theoretical study Yeh (1950) found that because the superposition of a vortex on a steering current is non-linear a tropical cyclone moving under the influence of a steering current should also describe a trochoidal motion. In a typical case his theory predicts oscillations with amplitudes from 40-80 km and periods of 2 to 3.5 days. After the publication of Yeh's work Horn (1951) presented tracks of typhoons Allyn 1949 and Doris 1950 which showed oscillations in low latitudes of periods 24 to 36 hours and amptitudes of 30-85 km. Such wavy or trochoidal tracks are much less frequent than either smooth or erratic tracks. When trochoidal oscillations are observed their period is usually much less than that predicted by Yeh. Additionally, Yeh's theory does not explain why only a few tropical cyclones exhibit the phenomenon. Kuo (1969) and Khandekar and Rao (1975) also studied this effect. The former found that the occurrence or non-occurrence of oscillations depends both on the vorticity of the vortex and on the steering current. Horn (1951) observed that the period of the oscillations tended to increase with time; Kuo (1969) considered that this was due to a reduction of storm vorticity as the size increased. Jones (1977a, 1977b) ran a numerical model of a tropical cyclone (without the beta-effect) with a basic current of 10 m s^{-1} . He found that the storm made trochoidal oscillations of period about 15 hours and amplitude about 15 km. The mean motion of the storm i.e. the motion without the oscillations, was about 5^{o} to the right of the mid-

tropospheric steering current. He also ran the model with a mature tropical cyclone and no environmental current and again obtained a trochoidal motion; this he related to the current in the outflow layer. The mean motion of the storm was about 70^{o} to the right of the outflow current.

The observed oscillations are most marked by movements of the eye and central regions of the circulation while the outer portions of the storm move on a more stable track. The oscillations are observed usually to have periods between about 6 and 48 hours and amplitudes between 30 and 200 km; they have been reported in several Atlantic hurricanes, notably Hazel 1954, Betsy 1956 and Carla 1961. The latter was observed by radar to make some six or more trochoidal loops. The famous Darwin cyclone Tracy (1974) was also observed by radar to make oscillations (Fig. 12.3) with period of about 8 hours and amplitude 6 km. In spite of the large number of typhoons and good radar coverage in the northwestern Pacific there have been relatively few oscillatory tracks reported from this area. Many radar time-lapse films have been made at Hong Kong but none has shown clearly defined, sustained oscillations. Small perturbations are difficult to determine objectively because of uncertainties in locating the exact storm centre at any instant. Changes in the shape and structure of the eye wall, as seen by radar, occur most of the time and often make the determination of the geometric centre more a matter of judgment than fact. If one discounts the difficulties and uses a little imagination it could be said that Fig. 10.28 shows two trochoidal oscillations between 121200 and 130900. However, such small oscillations are difficult to substantiate in the face of the uncertainty of the fixes.

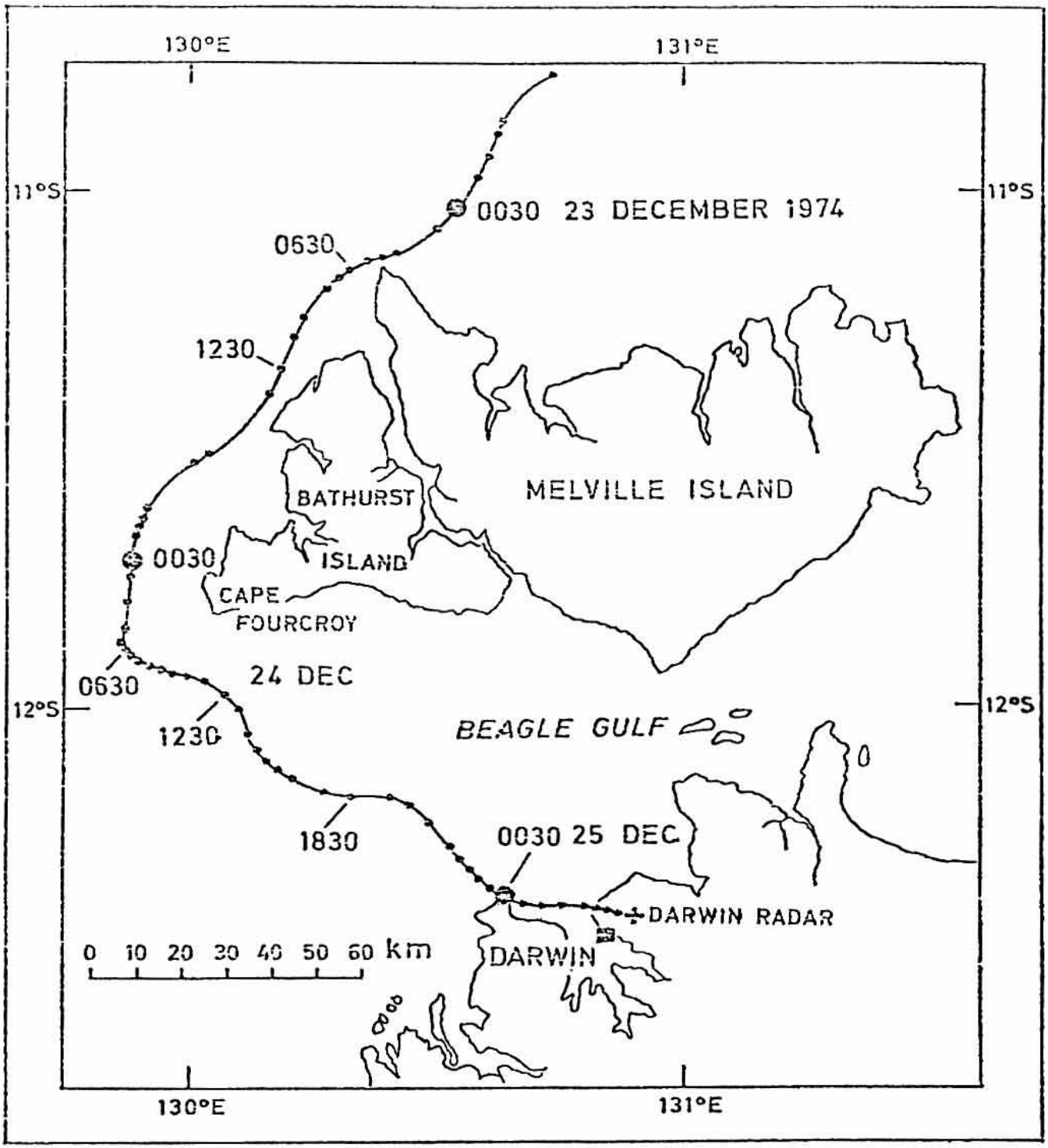

Fig. 12.3. The track of cyclone Tracy as determined by successive positions of the centre of the radar eye. (After Australian Bureau of Meteorology, 1977.)

Time-lapse films made from pictures of hurricanes taken at intervals of 30 minutes or so from geostationary satellites sometimes show the eye of the storm moving within the steadier cloud mass of the hurricane (e.g. Gladys, 1975). Lawrence and Mayfield (1977) produced the composite photograph of Fig. 12.4 to show two small trochoidal oscillations of hurricane Belle 1976 as determined from the GOES geostationary weather satellite. Each strip in this photograph was taken from an independently gridded, 8 km resolution, infrared image. The time of every strip is indicated on the right side and each is wide enough to show the eye. The central pressure minimum of the storm at this time (when it was about 500 km east of Florida) was 960 mb and its forward speed increased from 3.6 m s^{-1} to 6.2 m s^{-1}.

Although small oscillations are difficult to measure they are fortunately not significant from the operational point of view; the same cannot be said of the larger amplitude swings such are illustrated in Fig. 12.3. The track of Tracy emphasizes the point made of section 10.XX that a storm should be tracked for several hours before deciding on a mean motion. In the case of Tracy 1974 it was noted that the speed tended to be greater with track deviations to the left and less with deviations to the right. The speed of the centre along the track varied between 1.5 and 2.4 m s^{-1} whereas the mean speed was 1.8 m s^{-1}. Oscillations in the track of a tropical cyclone, like those in Tracy, cannot be predicted but they are important in determining where the storm will cross a coast. If they are in progress as a tropical cyclone approaches a coastal community or installation a prudent forecaster would have to make allowances both for their continuation and their cessation.

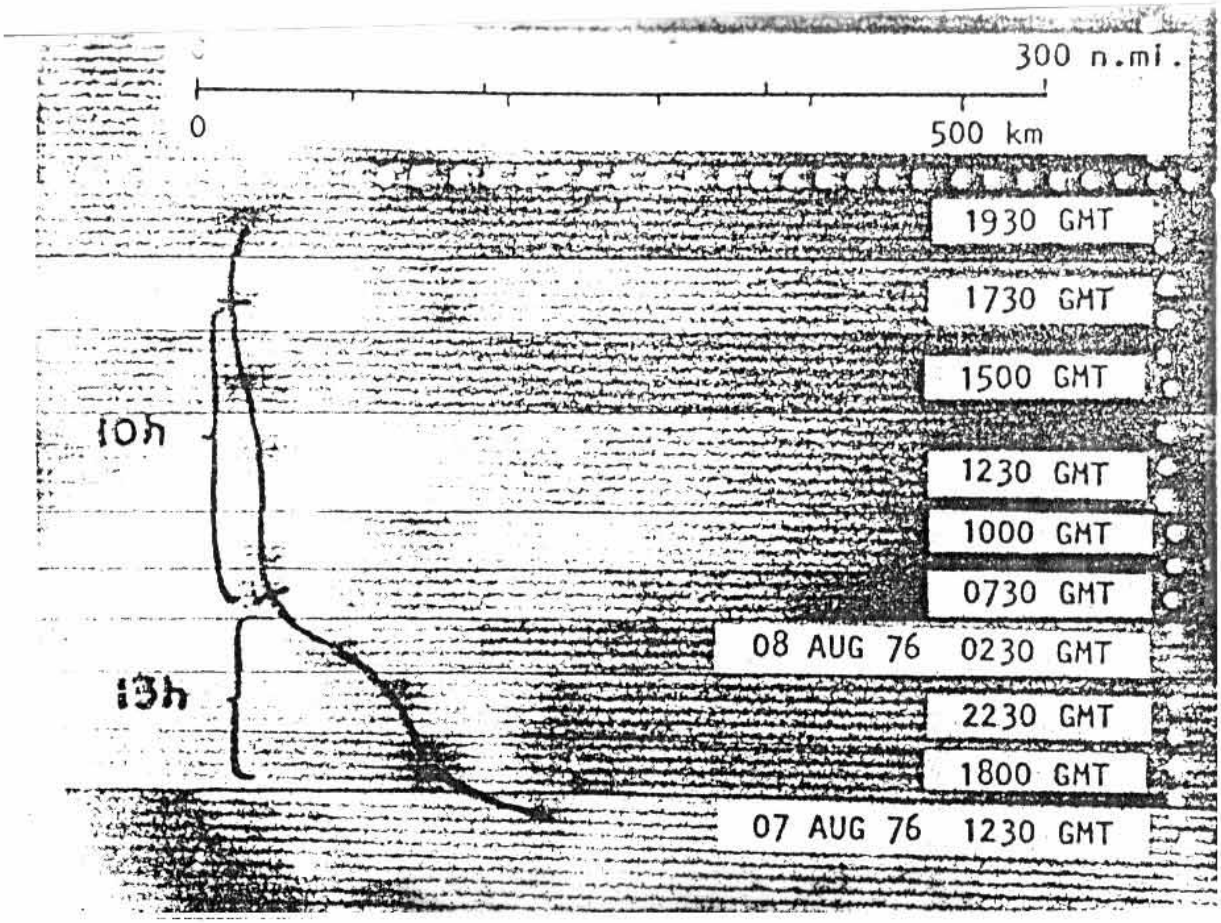

Fig. 12.4. Strips from GOES geostationary satellite infrared pictures of hurricane Belle 1976 showing the eye at times indicated. (From Lawrence and Mayfield 1977).

12.3.4 Frictional Effects

Dunn, et al. (1955) and Imai (1963) noted that Atlantic hurricanes and Japanese typhoons respectively, often veer to the left on crossing a coast (see Fig. 10.27). Dunn, et al. (1955) attributed this effect to the retardation of the winds in that part of the storm which was over land. Rao (1970) made an analytical study of the short term effects of differential friction on an axisymmetric vortex moving on a coast. He found that accelerations arise from an asymmetric redistribution of divergence such as those attributable to the beta-effect; however, the latter depend both on intensity and size of the vortex while the differential friction effects were found to be dependent only on the intensity of the circulation. His results indicate that if the eastern (western) half of the vortex lies over land its WNW movement due to the beta-effect is increased (reduced). If the northern (southern) half is over land the vortex moves westward (northwestward) at about 2 m s^{-1} . These results presuppose that there are no other influences present but, in general of course, there will be displacements due to large scale flow and there will be asymmetry in the tropical cyclone circulation. Furthermore, the formulation of the frictional stress in this model was grossly over simplified. However, Rao's results are not incompatible with a short term (about 6 hours) deflection to the left in certain circumstances particularly when the storm is intense, near axisymmetric and moving under a weak steering current. A slow-moving tropical cyclone will be under the influence of any differential frictional effect for a longer time than a faster moving storm; it is therefore less likely that any significant deflection will be observed in fast moving storms.

Brand and Blelloch (1973, 1974) studied the effects of Taiwan and the Philippines on the movement of typhoons which crossed them. It is not known what paths these typhoons would have taken in the absence of the islands, it is therefore difficult to assess their effect especially when individual tracks differ so greatly (Fig. 12.5). Brand and Blelloch considered that 24-hour forecasts of typhoon movement are heavily dependent on persistence and synoptic scale steering so that their errors - measured at right angles to the storm track - might be related to the effects of land which, being unknown, are not considered when making forecasts. They found that, on average, in the 24 hours before landfall on the islands typhoons tended to increase in speed and be deflected to the north. In the case of the Philippines the increase in average speed was from 4.5 to 5.5 m s^{-1} and the deflection to the north amounted to 34 km; for Taiwan the speed increase was from 5.5 to 6 m s^{-1} and the average deflection 33 km to the north. Storms leaving Taiwan were also observed to suffer an average southerly deflection of 96 km in 24 hours. The method by which these effects were determined suggests that they should be of value to forecasters but that further study is required to determine whether they are really caused by the islands.

In a numerical study of orographic effects on the path of a cyclone, Chang (1980) found that a cyclonic circulation was induced by the model cyclone moving westward and normal to the model island, which has am idealized topography similar to that of Taiwan. He suggested that the latent heat release is responsible for the establishment of the cyclonic circulation. On the other hand, surface friction does not seem to contribute to the deflection of the path of a cyclone.

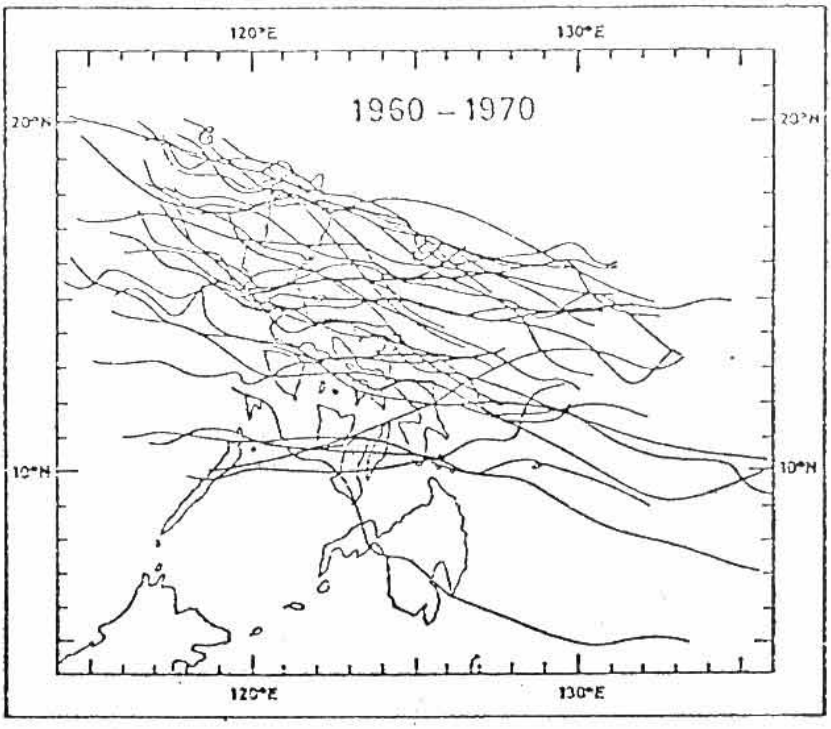

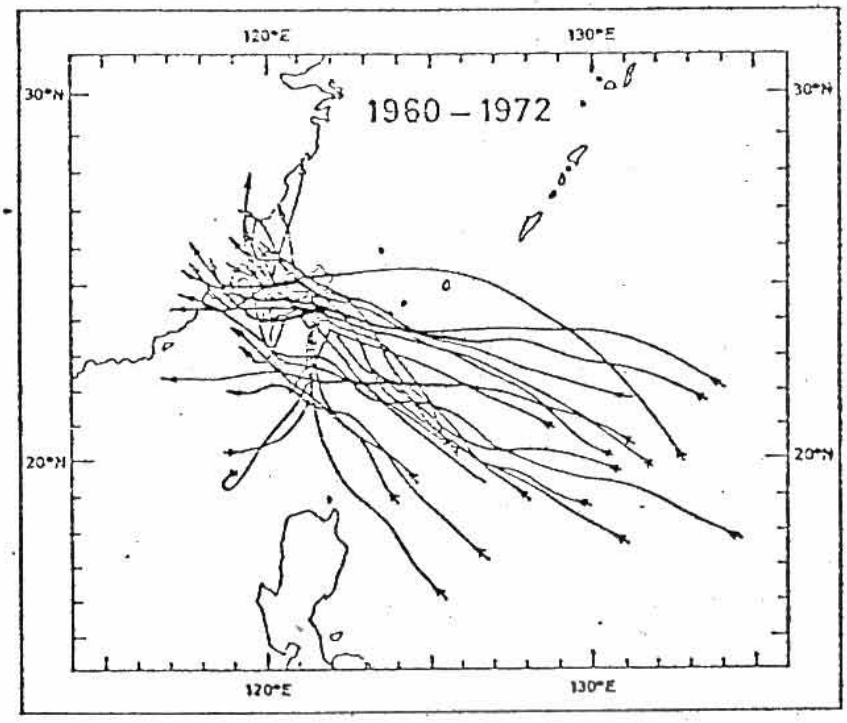

Fig. 12.5. Track segments for 30 typhoons crossing the Philippines and 22 typhoons crossing Taiwan. The tracks begin 48 hours prior to reaching the islands and end 24 hours after leaving them. (After Brand and Belloch 1973 and 1974).

This result seems to be rather surprising. It seems that the effect of the mountain is to weaken the low-level circulation of the cyclone by blocking the flow and inducing a leeside trough. In order for the cyclone to maintain its strength, extra energy must be generated, which is furnished in the model through cumulus convection. In doing so, a large-scale cyclonic circulation is induced, which then causes the cyclone to move northward. Whether this is actually the scenario in the real atmosphere is not certain. A more realistic boundary layer must be used in the model to represent the changes in sensible and latent heat fluxes when the cyclone encounters the topography. The effect of friction on dissipating the energy of the system must also be studied further. Observational studies must also be made to study the energy budgets of cyclones that cross the islands to determine the frictional and orographic effects on the path and intensity of the cyclones.

12.4 Directional Change

Most tropical cyclones form south of the subtropical ridge. Their initial motion therefore is, in general, westward or west-northwestward. However, as they progress towards the west, they will come under the influence of other synoptic flow features in the tropics and in the mid-latitudes. Thus, during the lifetime of a tropical cyclone, one or more changes in its direction of movement is often observed.

The most common directional change is known as recurvature, in which the cyclone starts to move to the right of its present direction. This motion has therefore also been described as right-turning. Most of this section will be devoted to this phenomenon. Another type of directional change which is not as common, and thus is seldom discussed in detail, is when a cyclone moves to the left from its current direction. This type of motion is described by Chan et al. (1980) as left-turning. Knowledge of the synoptic features associated with these two types of motion is very important because these directional changes are the most difficult to forecast. In the northwest Pacific, Burroughs and Brand (1973) showed that the average 24h forecast error for recurving typhoons is 252 km compared with 212 km for non-recurving typhoons. Chan, et al. (1980) fund that in the Atlantic, average 24h forecast errors for left-turning and right-turning cyclones are 289 km and 324 km respectively while for cyclones with no appreciable directional change, the corresponding error is 169 km.

A third type of directional track change is looping. This is the case when one part of the cyclone track intersects with another part of the track at some other time -- thus displaying a loop on the track chart. This type of motion is usually associated with weak or rapidly-

changing steering currents or binary cyclones -- and will be discussed in Section 12.6.

12.4.1 Recurvature

A tropical cyclone is said to "recurve" when, as a result of encountering the polar westerlies, its motion changes from poleward and westward to poleward and eastward. This change usually occurs relatively smoothly as in the classic "parabolic" paths of Fig. 12.2. However the change can be abrupt as when a typhoon stops after a normal west-northwest movement and then moves off directly towards the northeast (Fig. 12.6b). Tropical cyclones may drift or be steered towards the north and east and then revert to a track with a component towards the west before finally coming under the influence of the polar westerlies. For example, tropical storm Susan 1972 several times moved towards the northeast before final recurvature (Fig. 10.26). To predict when and where a tropical cyclone will recurve is one of the most important and difficult problems facing a forecaster.

Recurvature arises because the normal poleward motion of tropical cyclones over the oceans (Section 12.3.1) eventually brings many of them under the influence of mid-tropospheric polar westerlies which then carry the storms away, usually at a relatively high speed, towards the east. The relationship of the westerlies to typhoon recurvature is illustrated, in a climatological sense, in Fig. 12.7 which shows the mean latitude of the Pacific ridge at 500 mbar between 120° and 130°E in each month and the annual march of the mean latitude of recurvature.

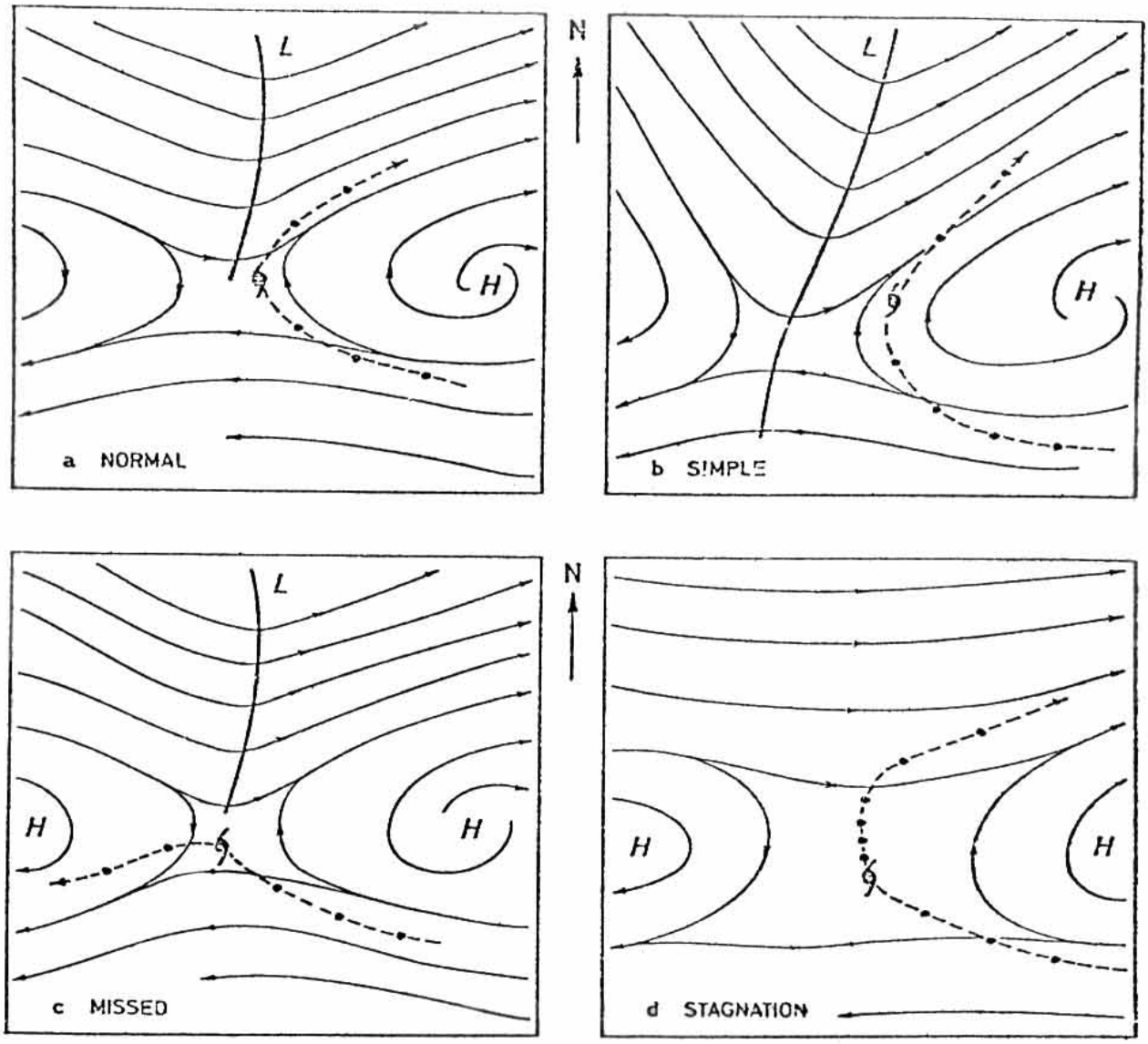

Fig. 12.6. Idealized diagrams illustrating the 500 mbar streamline patterns associated with common recurvature situations and a case of missed recurvature.

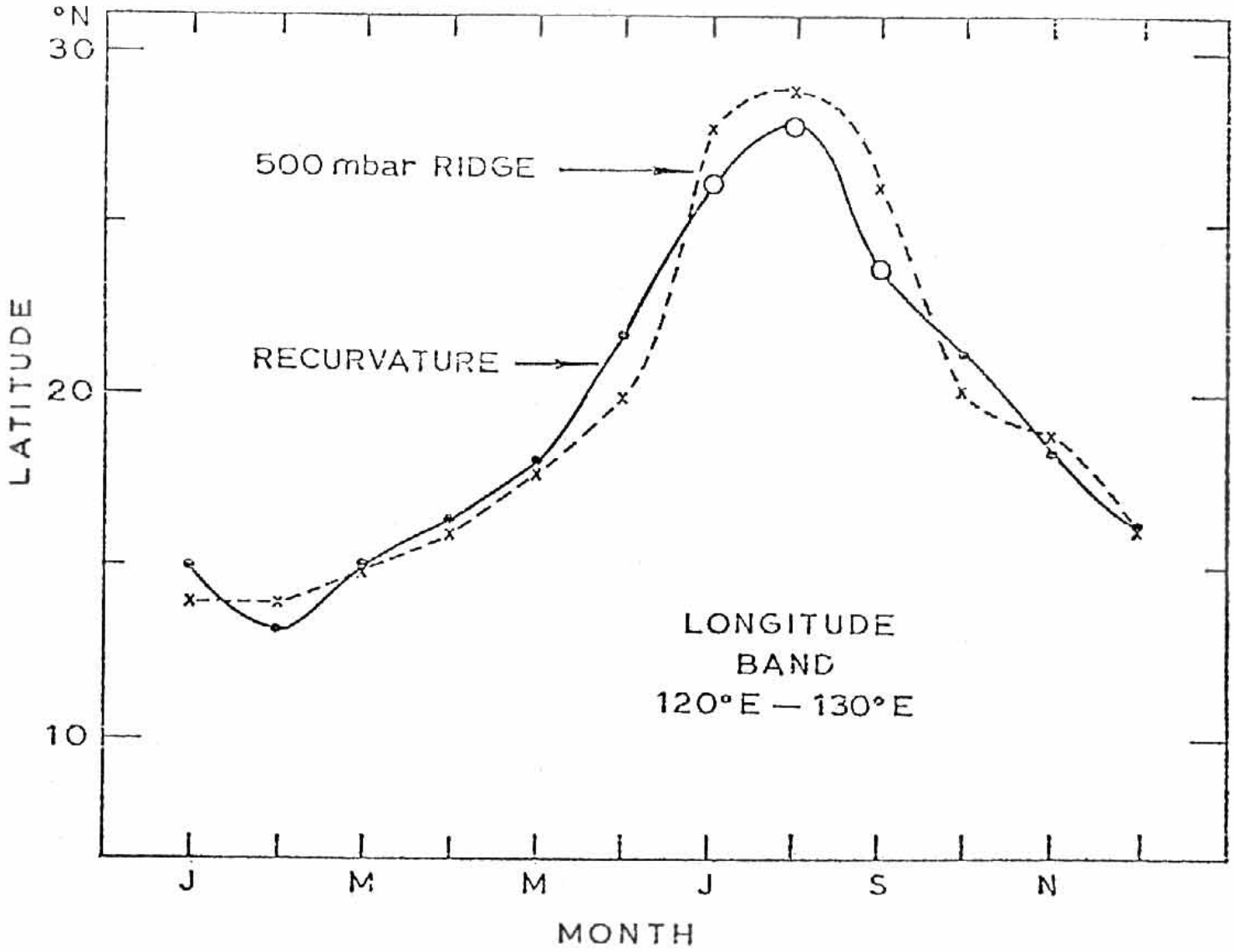

Fig. 12.7. The latitude of the mean 500 mbar ridge over the Pacific Ocean between longitude 120° and 130°E (from Fig. 3.XX) and the mean latitude of recurvature in the same area for each month. The mean latitude of recurvature has been obtained from tracks for the period 1884-1970 except that the open circles refer to the period 1947-1970 because early R.O.H.K. charts did not extend north of 30°N.

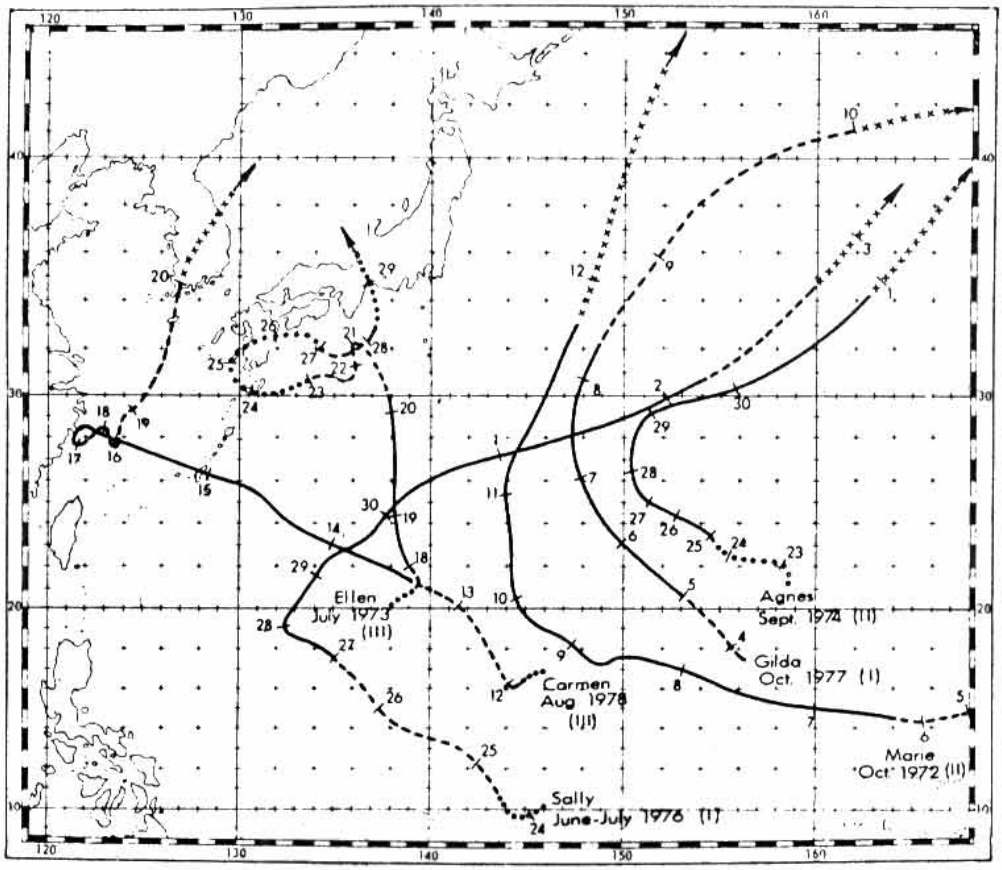

Fig. 12.7. Illustration of three common types of recurving typhoon tracks. See text for discussion of types (from Bao and Sadler, 1983).

Once north of the ridge the typhoon becomes embedded in the mid-tropospheric polar westerlies. On some occasions the process can be interpreted as the movement of the typhoon around the ridge from the Pacific anticyclone as illustrated in Fig. 12.1 and Fig. 12.2b. However, this interpretation usually entails looking at one particular level or pressure surface because, in general, the ridge slopes with height (see Fig. 3.24) and has different latitudes at different levels and may even be non-existent at some levels as seen in Fig. 12.2a. Recurvature is therefore a special case of steering and its prediction has all the attendant difficulties of identifying the steering currents and predicting their change.

Early work on the recurvature of tropical cyclones e.g. Bowie (1922) and Mitchell (1924) was, of necessity, based mainly on surface charts and could not therefore take full cognizance of the contribution to steering from the flows at upper levels. However, some rules developed from this early work still stand but others remain current today only because some non-specialist texts have not taken account of the knowledge gained in the post-war years. One of Mitchell's (1924) rules which is well known is that "Any tropical storm will recurve into a trough of relatively low pressure that may exist in the same region where the tropical storm arrives". Riehl (1954) pointed out that many tropical cyclones do not so recurve even when surface conditions seem very favorable. Mitchell also wrote that a storm will not recurve until relatively low pressure has developed to the northward. Riehl (1954) subsequently noted that "some cyclones even force their way poleward through high-pressure areas". It was Riehl and Shafer (1944) who first gave sound rules for recurvature based on conditions in the upper-air.

They found that if, to the west of a westward-moving tropical cyclone, the base of the polar westerlies lowers to about 500 mbar in connection with an eastward-moving mid-latitude trough and is maintained there, then the storm will begin to recurve when the edge of the westerlies is about 1000 km to its west (illustrated in Fig. 12.6b).

Dunn and Miller (1964) gave three flow patterns as being associated with recurvature of tropical cyclones. They do not state explicitly to which level they refer but by implication it is the mid-troposphere or 500 mbar level. The patterns are:

1) large-amplitude troughs, extending southward from the westerlies and located within a few hundred kilometres to the west of the tropical cyclone centre (Fig. 12.6b);

2) well marked low-latitude troughs building northward into the westerlies; and

3) weak troughs between two separate high cells (Fig. 12.6a). The second flow pattern is infrequent in the northwestern Pacific and the author has been unable to find an unambiguous case to illustrate the effect.

Dunn and Miller (1964) also gave the following flow patterns as being associated with non-recurvature:

1) a strong subtropical high to the north of the storm with a major trough in the westerlies located far to the west of the storm;

2) westerlies zonal, i.e. waves having very small amplitude, and found at their normal latitudes or further north.

Burroughs (1973) stated that a prerequisite for the occurrence of recurvature was a weakness in the ridge to the north of the storm at all levels (in the troposphere). Such a weakness allows a tropical cyclone to move northward to interact with the westerlies.

Four frequent recurvature situations are illustrated by the idealized diagrams shown in Fig. 12.6. These diagrams are schematic because firstly, the streamline charts are assumed to remain unchanged during the movement of the typhoons which, typically, would last several days and secondly, the typhoon is shown only as a point. In practice, of course, the patterns change as the waves and anticyclones move or change intensity. Furthermore, in a real situation, the typhoon circulation often obscures the background flow pattern. Finally, but importantly, the illustrations refer to only one level in the troposphere - 500 mbar - whereas there are usually significant differences between the flow patterns at different levels each making its own contribution to storm motion. Nevertheless, the diagrams broadly illustrate the nature of recurvature and give some idea of the problems involved in its prediction.

The frequent recurvature situation in which a typhoon moves northward to the east of a trough in the westerlies and comes under its influence is shown in Fig. 12.6a. In Fig. 12.6b a deep trough to the west of the centre indicates, as already discussed, certain recurvature provided that the pattern remains steady. In Figs. 12.2b, 12.6a, and 12.6b the typhoons can also be considered as moving around adjacent anticyclones, as a vortex pair. A missed recurvature situation is illustrated in Fig. 12.6c. This is a difficult case to predict because it is frequently not clear which of the four environmental flows will catch the typhoon. In practice, the problem is further complicated because the trough may deepen or regress and so catch the storm, or weaken or advance so permitting the typhoon to progress westward to the next anticyclone. At times, a fast-moving trough could cause a brief

northward motion of the typhoon. Then, after the passage of the trough, the typhoon would continue on its way westward, thus resulting in a looping motion. This type of cyclone movement has been studied by Xu and Gray (1982) and will be discussed in greater detail in Section 12.6. The case illustrated in Fig. 12.6c differs from that in Fig. 12.6a only in the position of the typhoon relative to the trough in the westerlies. In Fig. 12.6d the typhoon has moved out of the trades into a "no man's land" between easterlies and westerlies. It is usual then for the storm to drift slowly poleward at a rare dependent on its size, intensity and latitude (Table 12.2 and 12.3) until, after what can be several days, it finally comes under the influence of the westerlies. During the days of drifting it is possible for the large scale Northern Hemispheric flow patterns and those around the typhoon to change greatly so that the outcome in a real situation might be different from that indicated. Very large errors of 750 km or even more can result in 48-hour forecasts of position if the prediction of recurvature or no recurvature is incorrect.

Based on actual tracks of northwest Pacific typhoons between 1970-1979, Bao and Sadler (1983) have classified recurvature (from a total of 71 cases) into three common types:

Type I: The motion of the typhoon changes uniformly from west-northwestward to northeastward (similar to those in Figs. 12.1 and 12.2). This type accounts for 70% of all the recurved typhoons in the sample.

Type II: The northward motion of the typhoon persists for one to two days before the typhoon moves towards the northeast. Fourteen percent of the sample falls in this category.

The flow pattern in this case is schematically portrayed in Fig. 12.6d.

Type III: Erratic behavior during recurvature in the form of looping, stalling. This could last for a few days. The typhoon could also weaken to tropical storm intensity. A total of 11 cases (16%) is found to belong to this category.

Examples of these three types of recurvature tracks are given in Fig. 12.8.

Actual weather charts illustrating simple recurvature, missed recurvature and stagnation before recurvature are shown in Figs. 12.9 and 12.10. The lower charts are normal streamline charts for the 500 mbar level and, for each case, refer to times 24h apart. The upper charts are known as "space-mean charts" in which the height at a point is determined by averaging, in a special way, the surrounding heights out to about 800 km. In this way the contours of the pressure surface are smoothed. In addition, the typhoon is removed by drawing a circle around it of such a radius as will just include the outermost-closed contour and entering at the centre the average of the heights on the circle at the four cardinal points. The broadscale flow or steering current in the vicinity of the typhoon at chart level can then be estimated and the likelihood of recurvature assessed. In Fig. 12.9 typhoon Kim is seen to be progressing westward to the southwest of the Pacific ridge and north of a low pressure area on the 13th November 1977 but, a deepening trough is approaching from the west. The trough meets Riehl's criteria for recurvature and causes Kim to turn northward when

Fig. 12.8. Illustration of three common types of recurving typhoon tracks. See text for discussion of types (from Bao and Sadler, 1983).

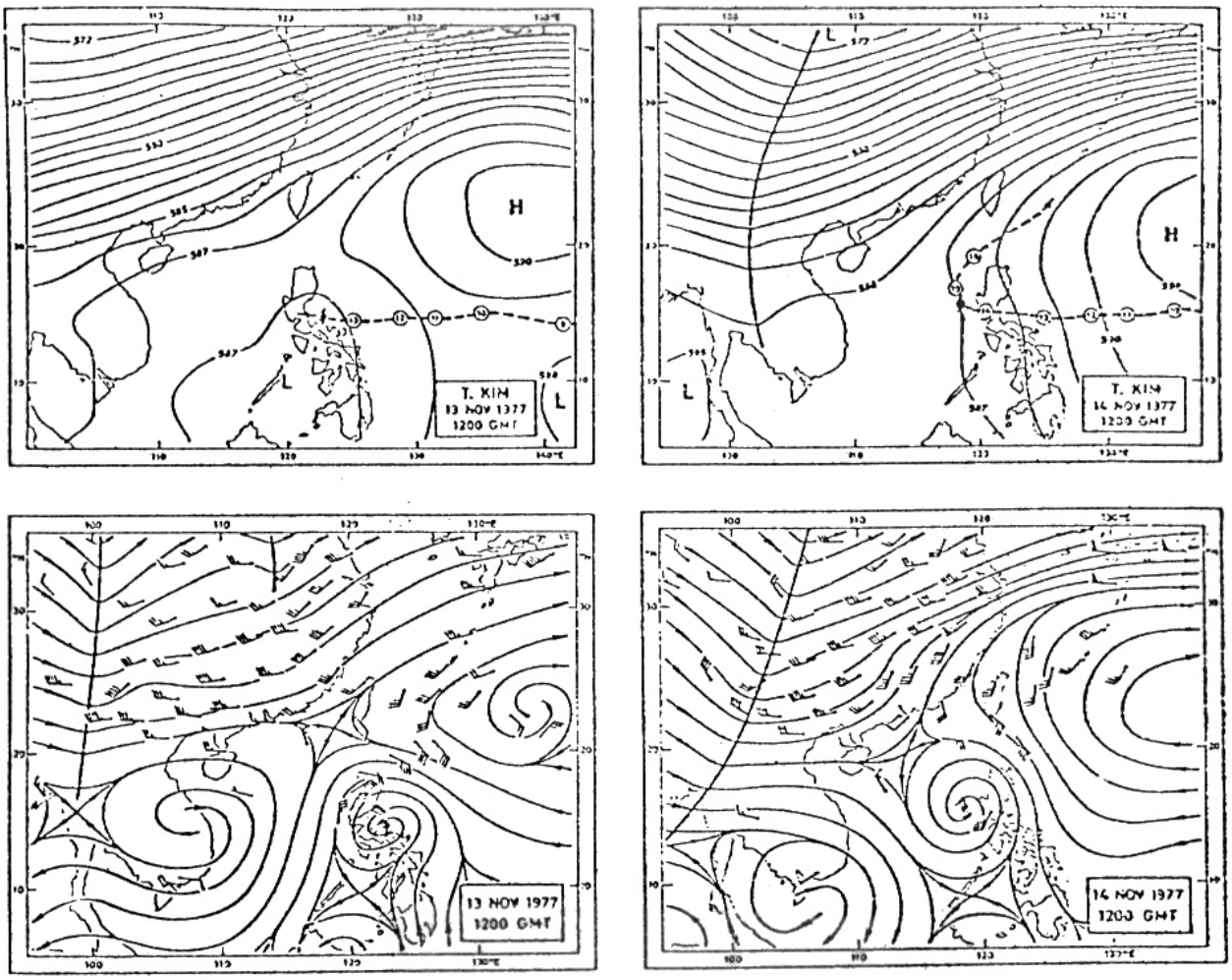

Fig. 12.9. The upper charts show computer-produced space mean charts for the 500 mbar surface with the typhoon's height field removed (contours are marked in dam). Normal hand-drawn streamline charts are shown below. Typhoon Kim's track illustrates a case of simple recurvature.

still about 1,600 km away. Note that in the streamline field the typhoon "meshes" with anticyclones to the east and west but that the weak western anticyclone appears as no more than a col in the smoothed height field.

The case of Typhoon Della shown in Fig. 12.10a is less clear cut. From the streamline chart for the 22nd October recurvature would not be expected in the short term because of the weak ridge to the north of the centre. However, with the approach of the short-wave trough in the westerlies the two troughs might reinforce and deepen and the ridge would then most likely collapse. In addition the Fujiwhara effect (section 12.5) between the two cyclonic vortices would tend to move Della towards the north - recurvature would then be possible. The space-mean chart presents a more positive picture of Della entering an area devoid of significant steering currents. The typhoon would be expected to remain near stationary while the trough continued eastward passing to the north of the typhoon. The charts 24h later show that this assessment was correct. Note again that on the streamline charts the weak anticyclone vortex over the Gulf of Tonkin and the weak cyclonic vortex near Ho Chi Minh appear as one anticyclone in the space-mean chart.

The case of tropical storm Amy shown in Fig. 12.10b is one of stagnation. The streamline chart on 20th August shows the typhoon to be larger than any nearby anticyclone and no major trough is in sight to the west. A very slow northward drift would be anticipated. The space-mean chart confirms this assessment as the heights at 10^{o} east and west of the centre are about equal. Twenty four hours later the storm had moved little. Subsequently, the trough continued its deepening

trend to the west of the typhoon which eventually recurved.

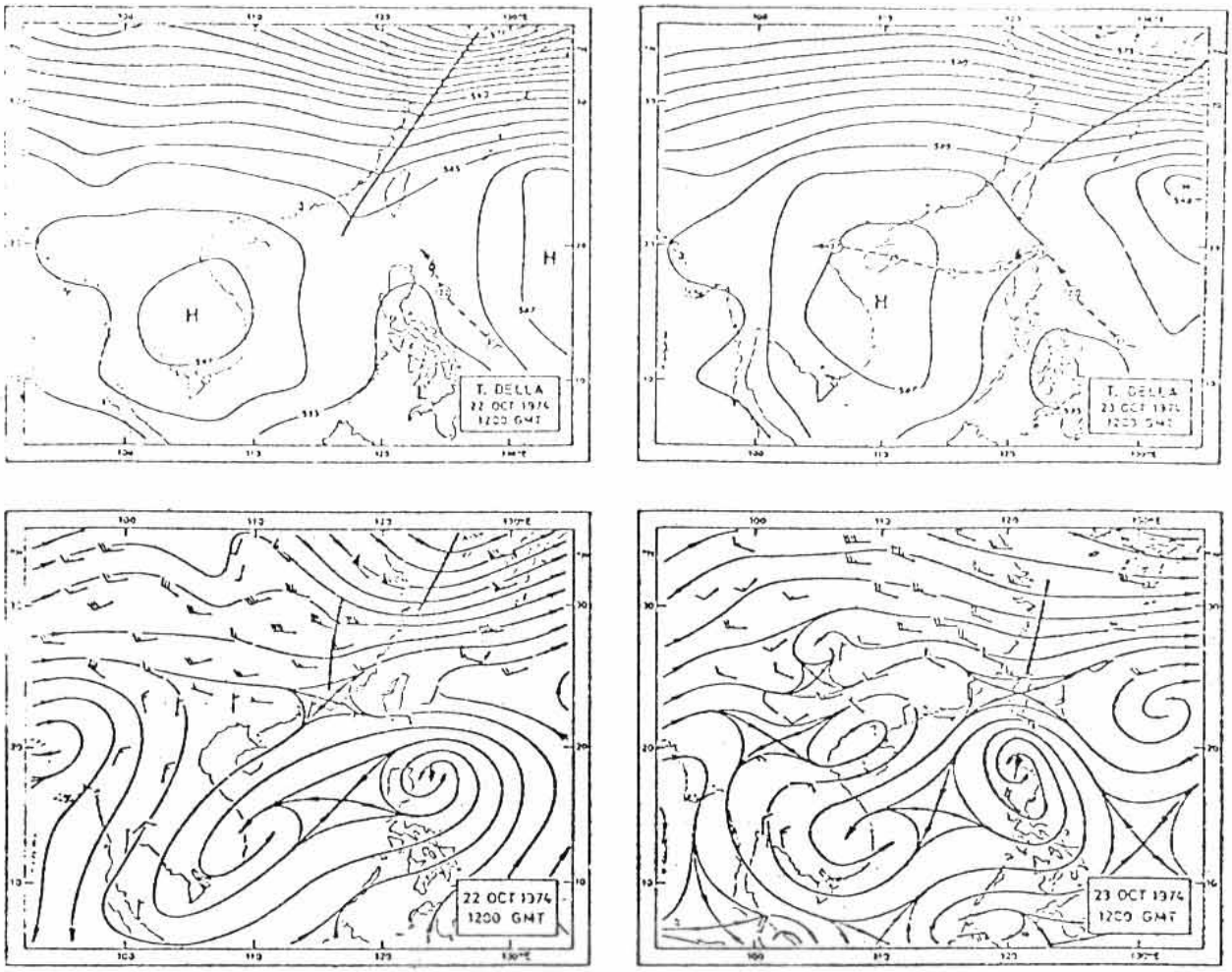

(a)

Fig. 12.10 a-b. Missed recurvature of typhoon Della (a) and stagnation of T.S. Amy prior to recurvature (b). Other particulars as in Fig. 12.9.

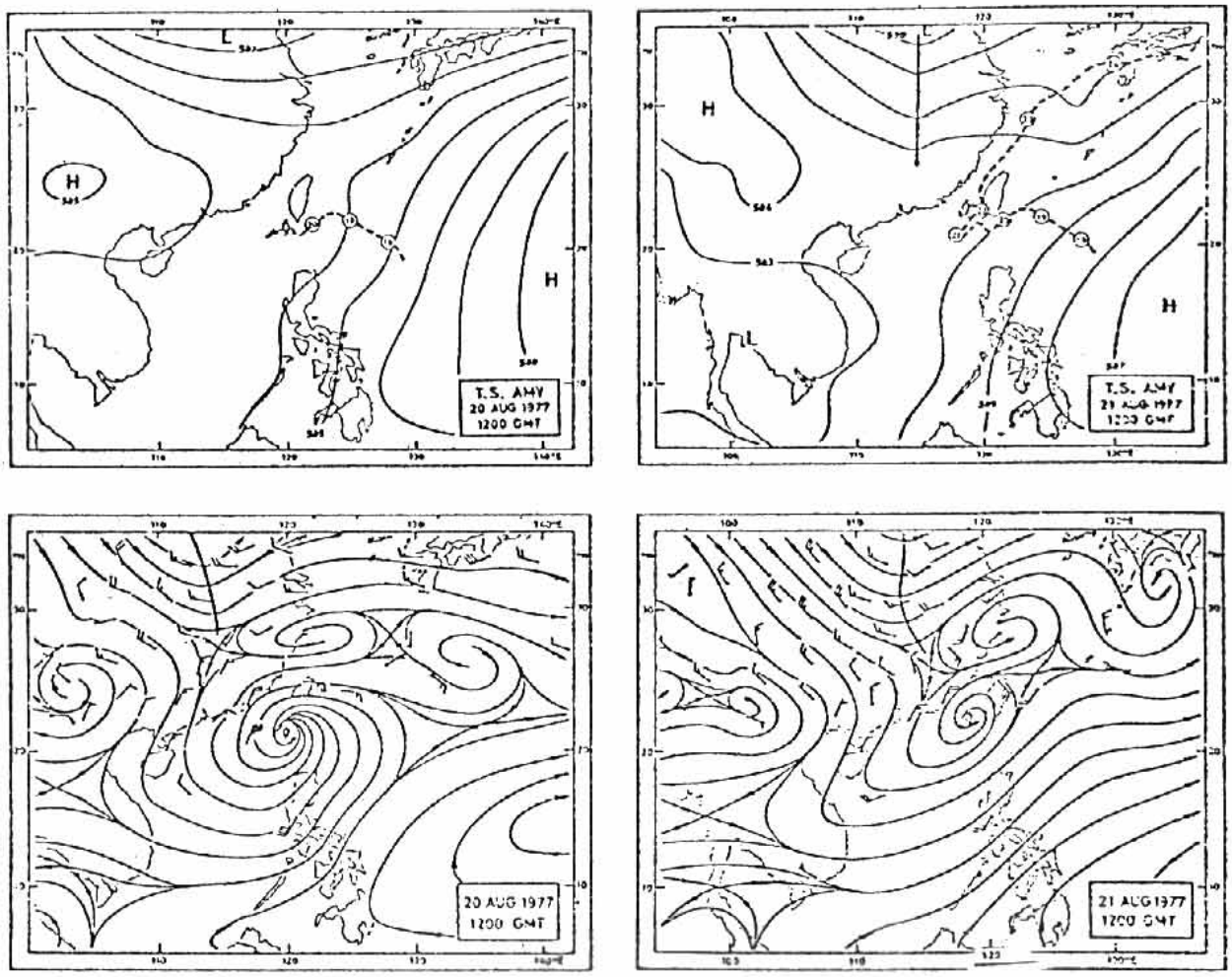

(b)

Fig. 12.10 a-b. Continued.

George and Gray (1977) chose 21 pairs of typhoons each comprising one storm which recurved and one from approximately the same starting position which did not recurve. The point where the recurving track acquires a northwesterly to northerly component and departs from the matched track was called the "S" point and is illustrated in Fig. 12.11. All rawinsonde data out to a radius of 21° latitude for the recurving and non-recurving storms were composited separately for various time periods before "S". In order to obtain adequate data the compositing was done not for a single observation time but for a 24h period. A composite chart for wind observations at a time 12h before S therefore included all observations from the time of S to 24h earlier. The first data points on the averaging grid are at a radial distance of 7° - 9° latitude (778 - 1000 km). It was found that the wind and height fields at 200 mbar for the recurving and non-recurving storms showed major differences as early as 60 h before the recurvature began at the "S" point. Composites of only 21 cases can be biased by one or two strongly abnormal cases and experience shows that several synoptic patterns are associated with recurvature so that, to some degree, the compositing process may be averaging "cows and sheep". Indeed, Guard (1977) has identified a summer and winter pattern for recurvature. Nevertheless, with the limitations of the method in mind, the composites display interesting features. In Fig. 12.12 is shown the composite of all wind observations a 700 and 200 mbar during the 24h prior to the time of reaching the "S" point. Streamlines have been drawn to fit George and Gray's mean winds to better show the main features. It can be seen that, at this time, the non-recurving storms show at 700 mbar, a

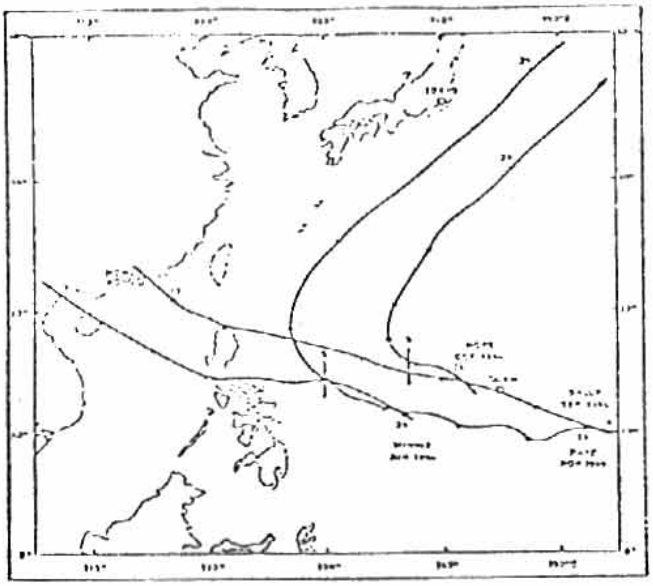

Fig. 12.11. Shows the location "S" at which two recurving typhoon tracks departs from those of two matched non-recurving typhoons.

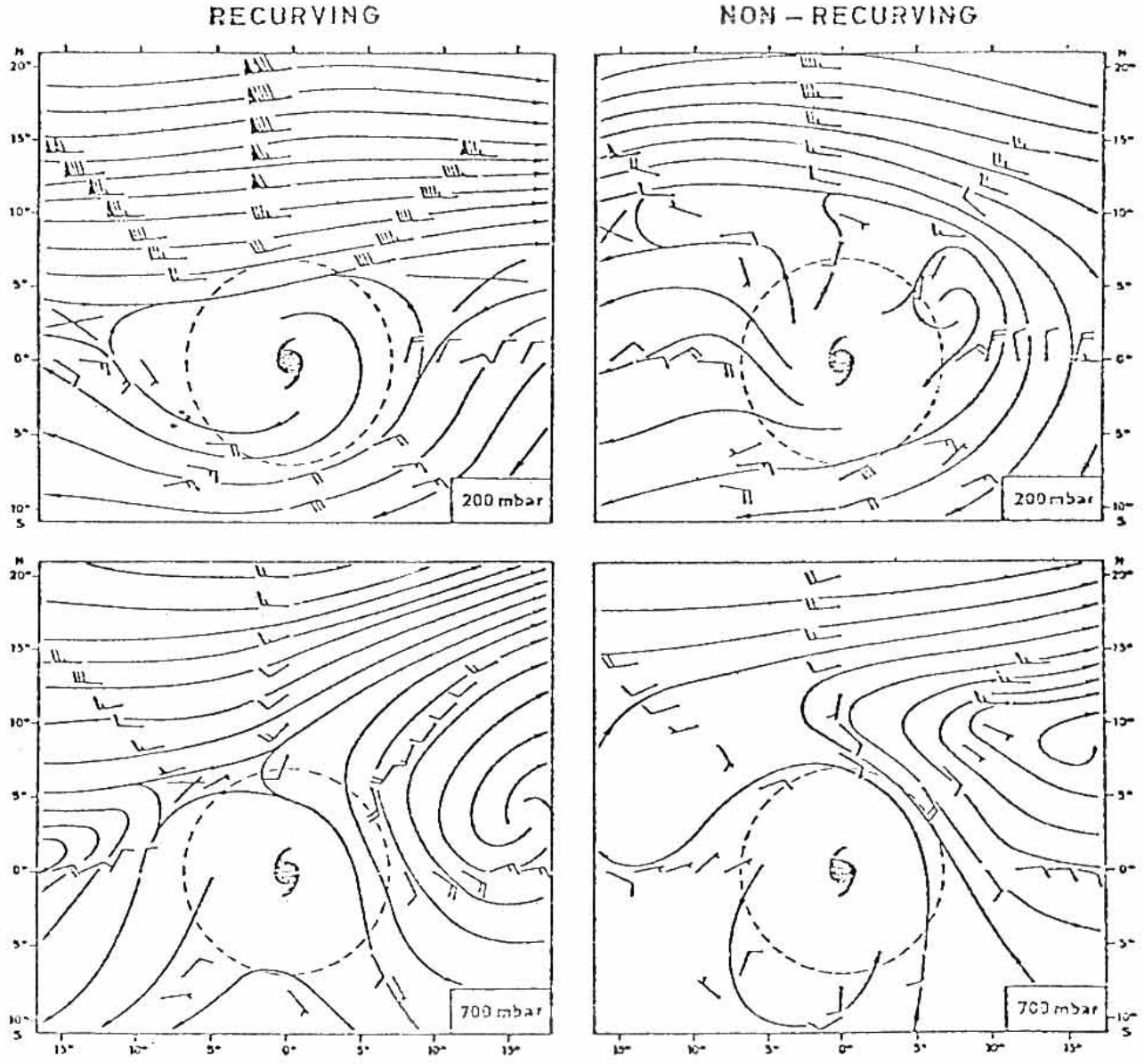

Fig. 12.12. Averaged winds at 700 and 200 mbar around 21 recurving typhoons (left) and a matched set of non-recurving storms (right), from George and Gray (1977). The observations refer to a 24h period centred 12h prior to recurvature (the "S" point in Fig. 12.7). Streamlines have been drawn to bring out the pattern.

strong ridge to the north whereas the westerlies come to within 1000 km of the centre in the recurving pattern. At 200 mbar the westerlies also come to within 1000 km of the centre of recurving storms but, the surprising feature is that the westerly winds at 20^{o} or 2200 km north of the centre are, in the recurving composite, some 35 m s^{-1} stronger than in the non-recurving composite.

In a rawinsonde composite study of the turning motion of tropical cyclones in the Atlantic, Chan, et al. (1980) also found a 500 mb flow pattern at the time of recurvature (or "right- turning" in their terminology) similar to the 700 mb flow found by George and Gray (1977). This is illustrated in Fig. 12.13.

Height differences between the recurving and non-recurving data sets of George and Gray (1977) are greatest at 200 mbar but temperature differences are greatest at 700 mbar as illustrated in Fig. 12.14. Chan, et al. (1980) also showed that the mean tropospheric temperature (between 1000–250 mb) is lower to the right-front (facing downstream of cyclone direction) of right-turning cyclones 24h prior to recurvature (Fig. 12.15). This relatively cold pool of air is also evident in the component of the vertical wind shear parallel to the direction of cyclone motion (Figs. 13 and 14 in their paper).

George and Gray (1977) further computed the changes in the recurving minus non-recurving geostrophic zonal and meridional wind across the storms at 12h and 36h before recurvature (Fig. 12.16). These

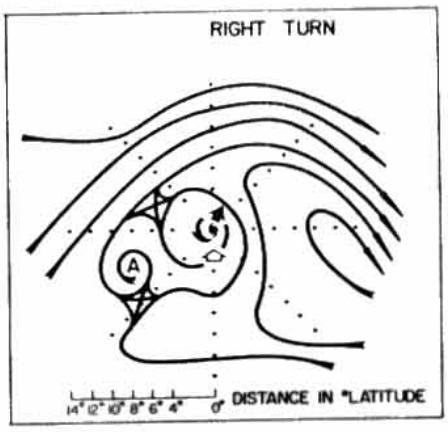

Fig. 12.13. Streamlines at 500 mb for Atlantic tropical cyclones undergoing a right-turning motion. The open arrow indicates the instantaneous direction of cyclone motion. The solid arrow represents the movement of the cyclone in the next 12h (from Chan, et al., 1980).

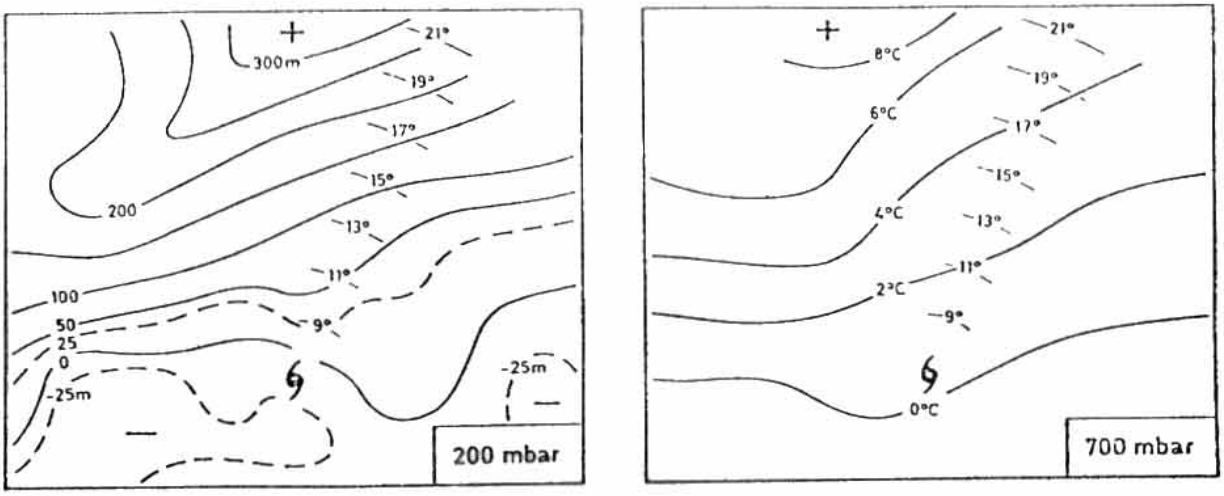

Fig. 12.14. The average height differences (m) at 200 mbar (left) obtained by subtracting the average heights for the recurving typhoon cases from those for the non-recurving cases. The 24h observation period is centred on 12h prior to recurvature (Fig. 12.11). The temperature differences at 700 mbar (right) were obtained in a similar manner. (Redrawn from George and Gray 1977).

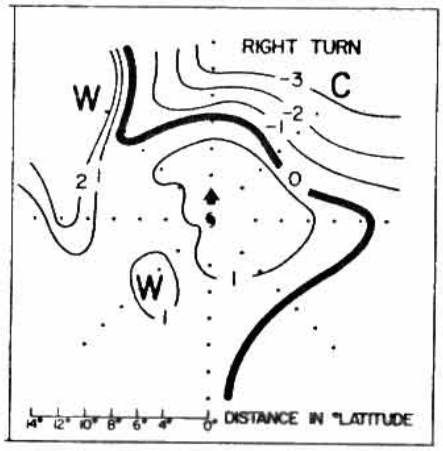

Fig. 12.15. Deviation of the 1000–250 mb layer mean temperature from the 5^{o}–15^{o} latitude radii average mean temperature for Atlantic tropical cyclones undergoing a right-turning motion. These data were derived from the Nimbus 6 microwave channel at 24h before the time of recurvature. The arrow at the cyclone center indicates the present direction of cyclone motion (from Chan, et al., 1980).

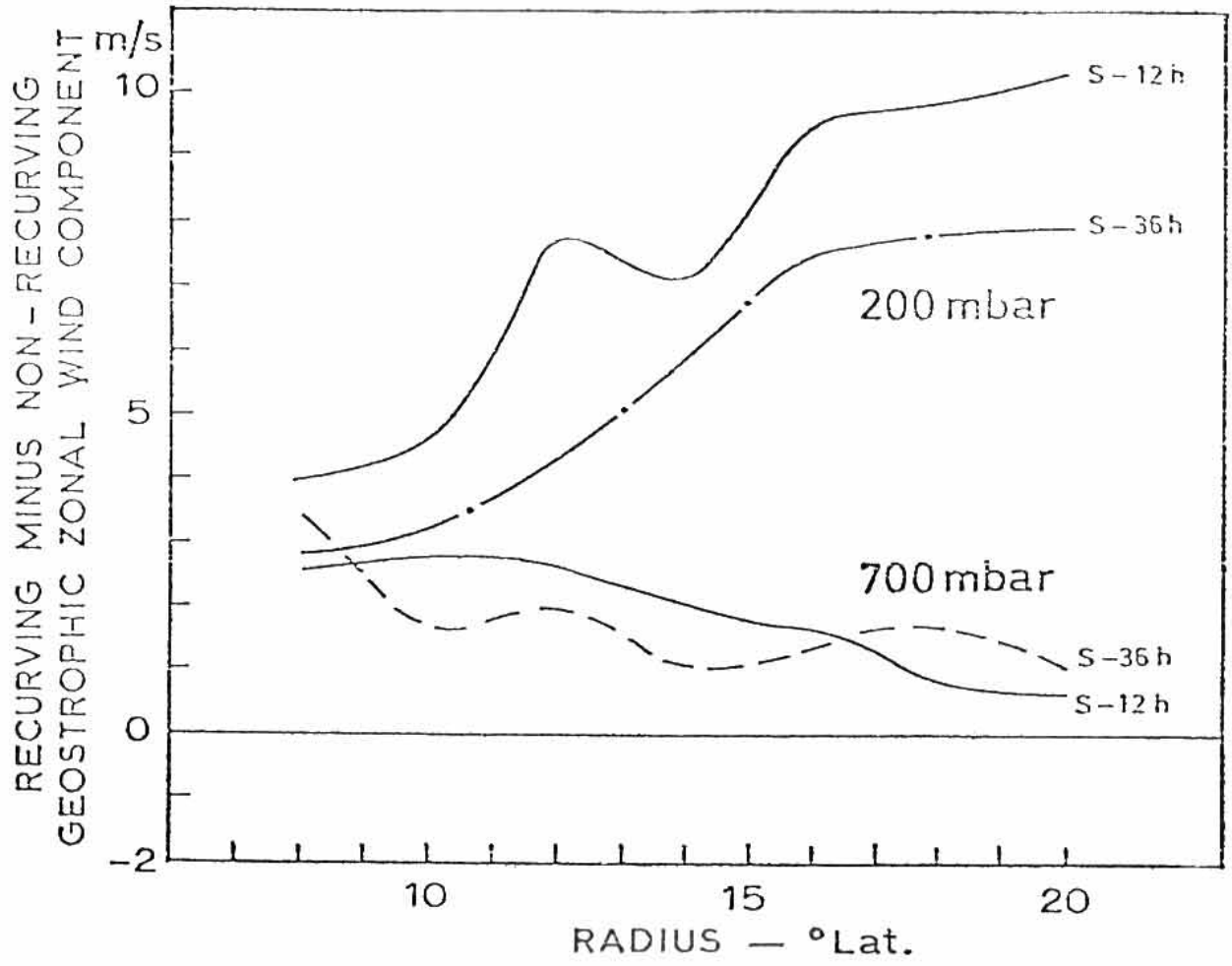

(a)

Fig. 12.16 a-b. The average geostrophic zonal (a) and meridional (b) wind component across recurving typhoons minus that across non-recurving storms at 700 and 200 mbar and at 12h and 36h prior to recurvature. (Redrawn from George and Gray 1977).

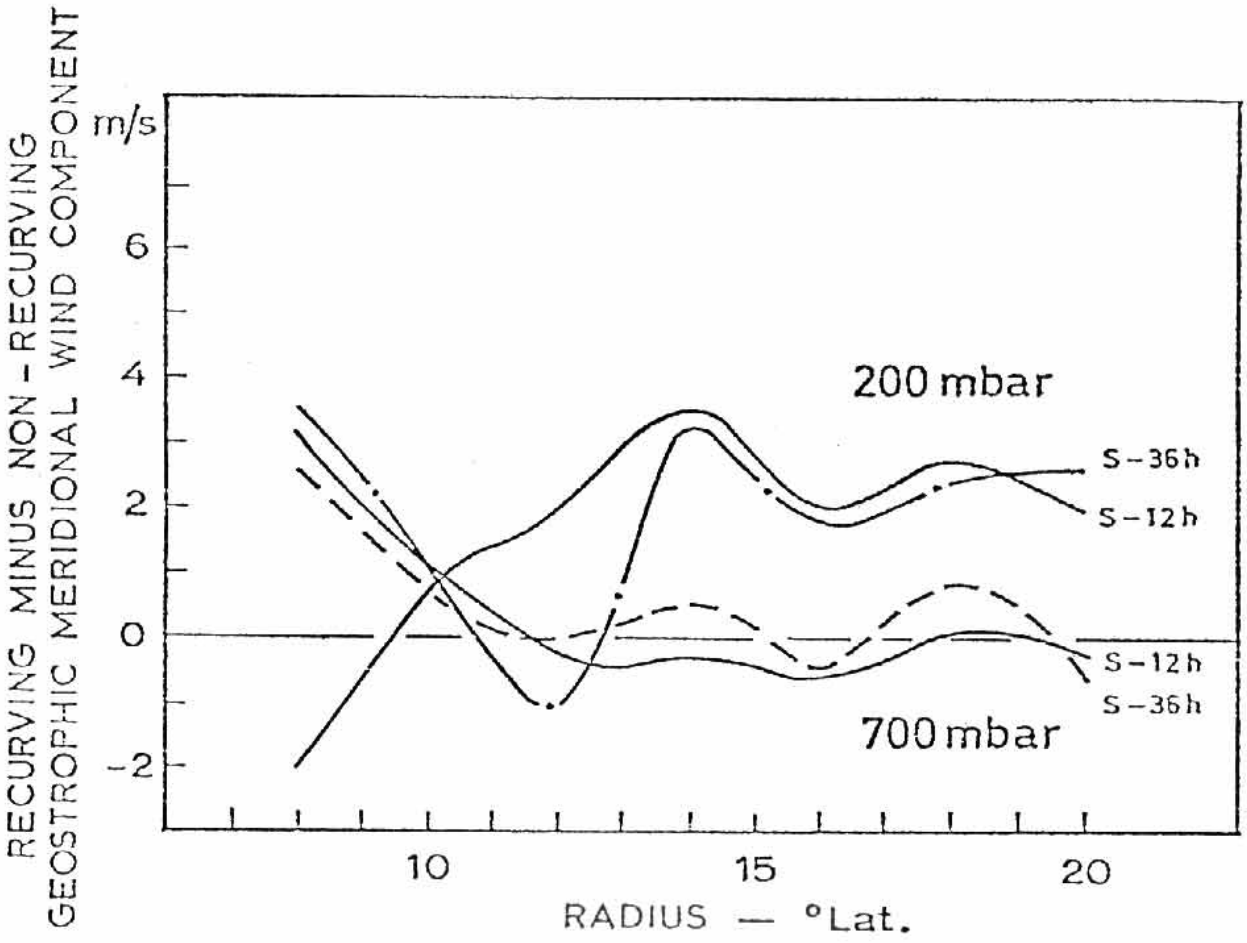

(b)

Fig. 12.16 a-b. Continued.

figures show that the greatest differences between the two types of storm are found in the 200 mbar zonal geostrophic environmental flow as measured across the typhoons from north to south at radii between 10^{o} and 20^{o} of latitude. The geostrophic component towards the north and the east for recurving typhoons is larger than that across non-recurving storms for both time periods shown.

12.4.2 Speed and Intensity Changes on Recurvature

Riehl (1972) examined a large sample of 66 recurving typhoons which remained over the ocean and met other criteria during the period 1957 to 1968. Within this sample (which amounted to nearly one-third of all typhoons in the period) virtually all typhoons reached their peak intensity - in terms of maximum wind speed - at, or a little before, the point of recurvature and subsequently weakened at a variable rate. The change in wind speed is normalized to the maximum speed observed. For example, if the maximum wind speed had been 60 m s^{-1}, a subsequent wind of 30 m s^{-1} would be given a normalized speed of 50%. In this way, Riehl was able to relate the decay of wind speed to the change in latitude of typhoons over the 48-72 hours after recurvature.

There were two categories of storms, those which did not move northward over more than 8° - 10° of latitude after recurvature are those which move further than this. In the first case the observations were well fitted to the straight line.

$$V_{max}/V_{o\ max} = 100 - 3.8\ (\phi - \phi_r) \qquad (12.2)$$

where V_{max} is the maximum wind speed at a given time and $V_{o\ max}$ the greatest maximum wind speed recorded in the life of the typhoons, φ the present latitude are φ_r the latitude of recurvature. The slope of this line had a standard deviation of 0.9.

For typhoons extending beyond 8° - 10° latitude after recurvature a logarithmic curve of the form

$$V_{max}/V_{o\ max} = 1/\ [1 + m(\phi - \phi_r)] \qquad (12.3)$$

fitted the data, where m is a constant. The mean curve for all typhoons which moved up to 16° north of φ_r is given in Fig. 12.17 where a

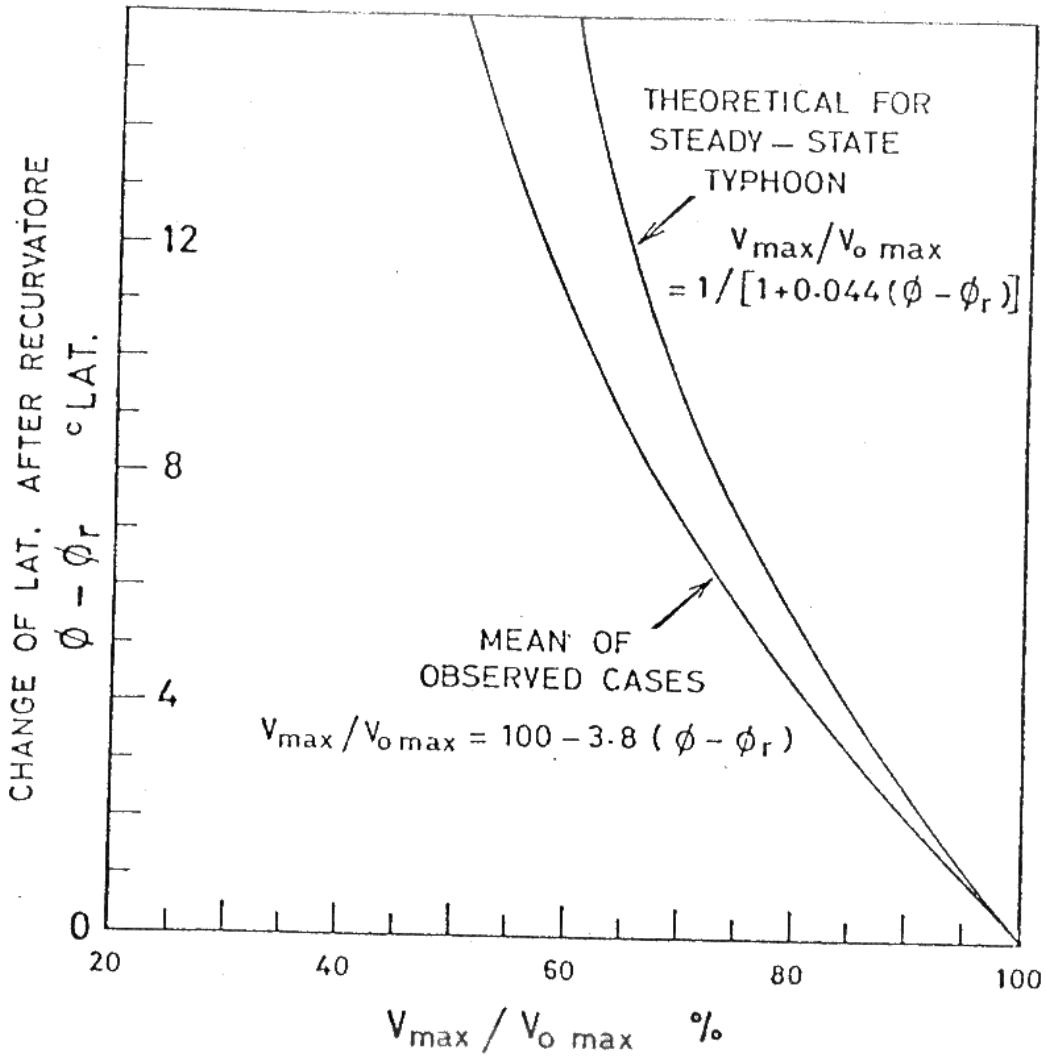

Fig. 12.17. The average observed and theoretical ratios of the maximum wind speed V_{max} in typhoons at a given time after recurvature to the speed $V_{o\,max}$ at recurvature, expressed in terms of the change of latitude from φ_r the latitude of recurvature. (Adopted from Riehl, 1972).

theoretical relationship is also shown. This curve wa derived on the assumption that the storms were in a steady state and that, as shown by Riehl (1963),

$$V_{max} = \text{Constant}/f \qquad (12.4)$$

where f is the Coriolis parameter. Using (12.3) and the approximate relationship $f = fo + \beta\ (\varphi - \varphi_r)$ where β is the change of Coriolis parameter with latitude, it is easily shown that

$$V_{max}/V_{o\ max} = fo/f = 1/\ [1 + \beta/fo\ (\varphi - \varphi_r)] \qquad (12.5)$$

A value of $\beta/f = 0.4 \times 10^{-6}$ per metre corresponding to 20^{o}N has been used in Fig. 12.16. The graph shows that a large fraction of the decrease in intensity of typhoons with latitude can be ascribed to the latitude effect but that an additional smaller term is present, which is possibly related to decreasing air and sea surface temperature northeastward.

Burroughs and Brand (1973) showed how the average speed of movement of typhoons increases after recurvature. They normalized the speed of movement to that at the point of recurvature. That is, they expressed the speed of movement as its ratio to the speed at recurvature. This ratio R_s is shown in Table 12.6 for each of the months May to December and at times up to 48h after recurvature. In general it can be seen that the average ratios increase with time after recurvature and increase from month to month during the course of the year. On the average, December storms accelerate so rapidly after recurvature that after 48h they are travelling nearly three times as fast as at recurvature. On average typhoons accelerated fastest when moving on

TABLE 12.5

Average monthly values of R_s (and standard deviation) as a function of time after recurvature for tropical storms and typhoons from 1945-69. The number of observations N is shown. (Adapted from Burroughs and Brand 1973).

	Time after recurvature											
	12h			24h			36h			48h		
Period	R_s	σ	N	R_s	σ	N	R_s	σ	N	R_s	σ	N
May	1.11	0.36	14	1.46	0.76	13	1.88	1.46	11	2.23	1.76	10
Jun	1.37	0.36	13	1.52	0.59	12	1.77	0.72	10	1.69	0.54	7
Jul	1.17	0.38	15	1.27	0.55	13	1.74	1.24	7	2.30	1.77	5
Aug	1.30	0.40	38	1.58	0.58	31	1.81	0.75	25	2.09	1.08	16
Sep	1.34	0.42	49	1.78	0.77	40	2.29	1.20	29	2.32	1.59	21
Oct	1.35	0.41	53	1.87	0.86	45	2.32	1.25	38	2.64	1.46	29
Nov	1.51	0.59	34	2.00	0.93	29	2.60	1.28	24	2.95	1.58	15
Dec	1.32	0.37	14	2.04	0.96	13	2.86	1.26	10	2.98	2.12	5

headings between 040° - 050° and attained the greatest speed on headings of 050° - 060°.

Table 12.7 shows the average values of the zonal (west to east) component of storm motion in five degree latitude bands for each of the months May to December. It will be seen that over all latitudes, this movement is lowest in August but jumps abruptly to the highest value in September. This increase is associated with, and is partially attributable to, an increase in the zonal flow of the upper westerlies as shown in Fig. 12.18.

Burroughs and Brand (1973) identified two basic synoptic situations associated with recurvature one of which led to a slower acceleration than average and the other to a more rapid acceleration. The faster acceleration occurs when a trough extends south of the latitude of the storm centre and moves to within 10° longitude west of the storm position (longitude of the trough measured at 35°N). The storm is then caught between the trough to the west and the ridge to the east (see, e.g. Fig. 12.9 bottom right) and as it becomes a short wave on the trough it recurves and its speed over the next 36h increases by more than average. These storms continue to accelerate as they become extratropical. The slower cases are associated with troughs which do not extend south of the storm centre (Fig. 12.10) but move to its longitude. The storm then drifts north for about 24h, merges with the trough and begins to recurve to the northeast with a 36h speed increase less than average. About 24h before becoming extratropical these storms show a sharp increase in speed towards the northeast.

Burroughs and Brand (1973) also noticed an effect which is found when typhoons occur in pairs, an event especially frequent in September

TABLE 12.6

Average monthly observed values of the zonal (west-to-east) component of the speed of movement as a function of 5° latitude bands for recurved tropical storms and typhoons from 1945-69. Averages are also presented for all months (May-December) and for all latitude bands combined. Speeds are given in m s^{-1} and the number of observations is shown in parentheses. (Adapted from Burroughs and Brand 1973).

	Latitude bands (°N)						All bands
Period	12.5-17.4	17.5-22.4	22.5-27.4	27.5-32.4	32.5-37.4	37.5-42.4	12.5-42.4
				m/s			
May	3.3(10)	3.3(65)	5.3(49)	6.1(31)	12.4(7)	0(0)	4.8(162)
Jun	0(0)	5.2(29)	6.0(45)	7.1(36)	6.3(22)	10.7(4)	6.3(136)
Jul	0(0)	5.1(2)	5.0(19)	5.1(36)	6.9(39)	7.1(15)	6.0(111)
Aug	2.5(2)	4.7(11)	4.2(26)	3.6(103)	4.6(129)	6.5(50)	4.6(330)
Sep	0(0)	2.7(20)	4.1(94)	6.2(119)	7.9(116)	10.9(44)	6.5(393)
Oct	3.7(14)	3.5(97)	4.1(178)	6.8(156)	8.3(88)	10.9(22)	5.7(555)
Nov	3.1(16)	3.6(91)	5.4(89)	6.4(67)	8.0(21)	8.7(3)	5.1(287)
Dec	3.2(21)	3.9(61)	5.0(32)	10.8(4)	18.1(2)	10.2(3)	4.7(123)
May-Dec	3.3(63)	3.7(376)	4.7(532)	5.9(552)	6.9(424)	8.7(150)	5.5(2097)

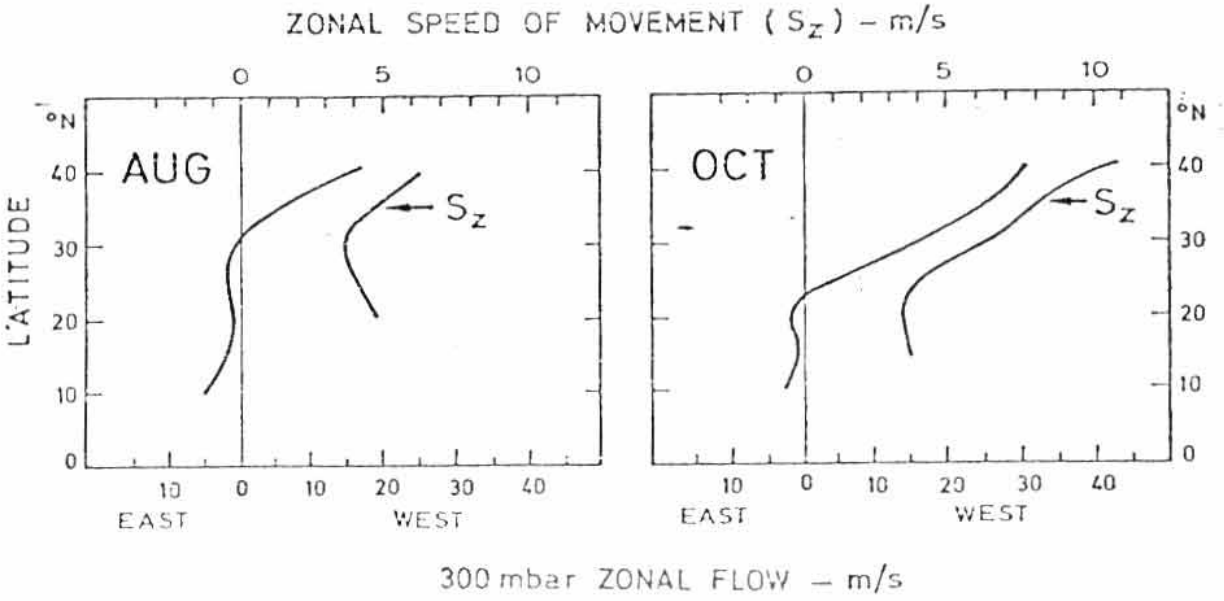

Fig. 12.18. The zonal (west to east) component of the speed of movement (S_Z) of recurved tropical storms and typhoons (1945-69) and the 300 mbar zonal wind speed, both plotted against latitude for the months of August and October. The wind speeds are for the longitude band 120° - 170°E. (Adapted from Burroughs and Brand 1973).

and October. The storms being considered are further apart than the 14° latitude or 1500 km distance at which interaction is expected (section 12.5). The first or most westerly of the storms is absorbed by a westerly trough as in the slowly accelerating storm case. It moves northward and northeastward and accelerates slowly. The storm to the east then begins to accelerate northward or northwest if the ridge is strong, and reaches speeds well above average. When recurving to the northeast the second storm can attain speeds two to three times those of the previous storm, at the same observation time.

In a study of recurved typhoons in the northwest Pacific, Bao and Sadler (1983) found a very good relationship between the speed of the typhoon after recurvature and the observed upper tropospheric wind at and before recurvature averaged between 500 mb and 200 mb along the subsequent track. However, since mid-tropospheric data are very sparse, they chose to correlate the speed after recurvature to only the observed winds at 250 mb. The results for 71 recurved typhoons (during 1962-1978) are shown in Fig. 12.19. Forecasts made using a dependent sample show an improvement of ~ 50% over the official speed predictions made by the Joint Typhoon Warning Center at Guam.

The discussions in these two sub-sections show that although considerable knowledge has been gained about recurvature over the years, a forecast of a right-turning motion still cannot be made with very high confidence. This is partly a result of the lack of data over the ocean so that the surrounding flow of the tropical cyclone cannot be well-defined. Satellite data may be able to fill part of the gap in the years to come. More studies must still be made to provide better objective criteria in determining possible recurvature. Present

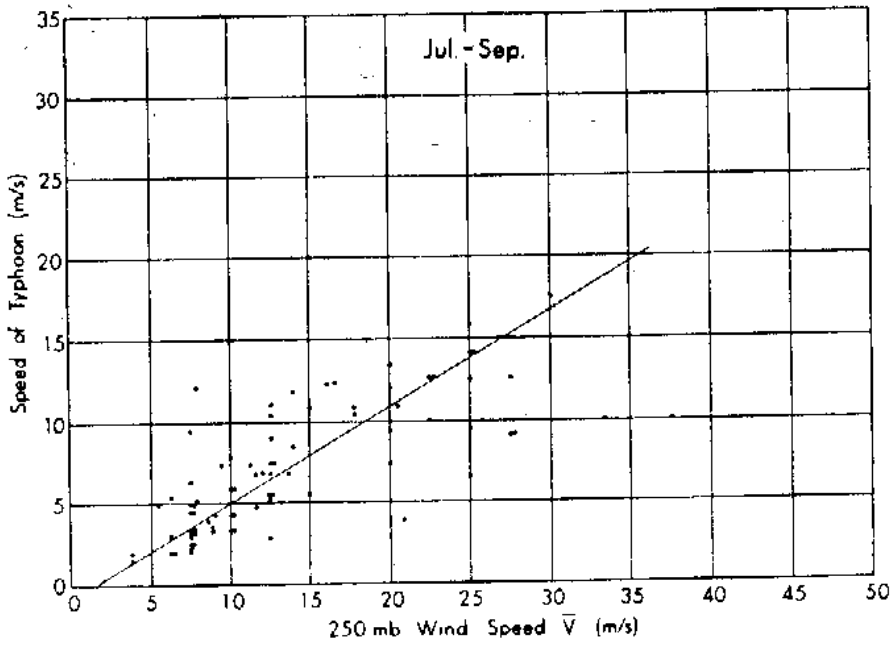

Fig. 12.19a. The average 250 mb wind speed at and 24h before recurvature at points along the typhoon track 24, 48, and 72h after recurvature, versus the speed of the typhoon at the same points and times. Data sample is 32 typhoons during July-September for the years 1962-78 (from Bao and Sadler, 1983).

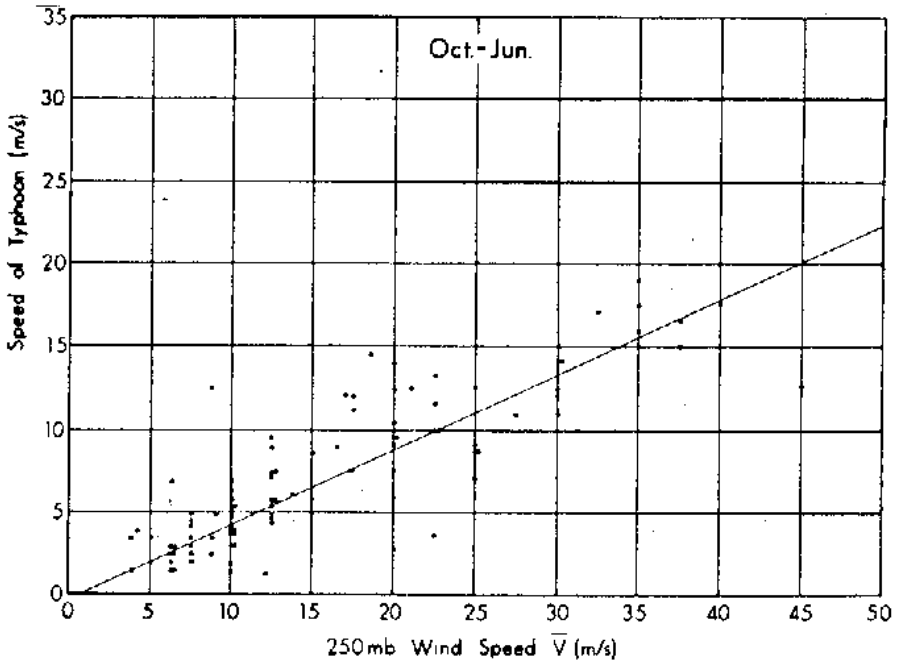

Fig. 12.19b. As in Fig. 12.18a but for 39 typhoons during October-June (from Bao and Sadler, 1983).

statistical and dynamical track prediction models must also be refined to reflect the improved understanding of the problem of recurvature.

12.4.3 Left-Turning

Because left-turning motion of tropical cyclones is a much less common occurrence than the phenomenon of recurvature, it has not been studied in great detail. Some examples of left-turning cyclone tracks in the Atlantic are shown in Fig. 12.20. In most cases of left-turning, the cyclone has a rather strong northerly or northeasterly component. Very seldom will a westward-moving cyclone change its course by veering to the left of its present direction.

A composite study of the large-scale features associated with left-turning cyclones in the Atlantic was made by Chan et al. (1980). They found that at the time when a cyclone starts to make a left-turn, the streamlines at 500 mb show a definite "cross- track" pattern, as shown in Fig. 12.21. An anticyclone is formed in front of the cyclone so that the steering flow "causes" the cyclone to turn to the left of its present course. In an analytical study, Chan (1982) explained the turning in terms of both vorticity advection by the flow and the coupling between the convergence of the vortex and the horizontal shear present in the surrounding flow. Chan (1984) found that this theoretical result is consistent with the computations of the vorticity budget from the data set used by Chan et al. (1980).

In terms of the mean tropospheric temperature, Chan et al. (1980) found that the atmosphere between 1000 mb and 250 mb to be relatively cold to the left of the cyclone (Fig. 12.21). From hydrostatic reasoning, an anticyclone must be present at the lower levels and a cyclone at the upper levels. Although Chan et al. (1980) did not

demonstrate this to be the case, Chen and Ding (1979) found that northward-moving cyclones have a tendency to turn towards an upper

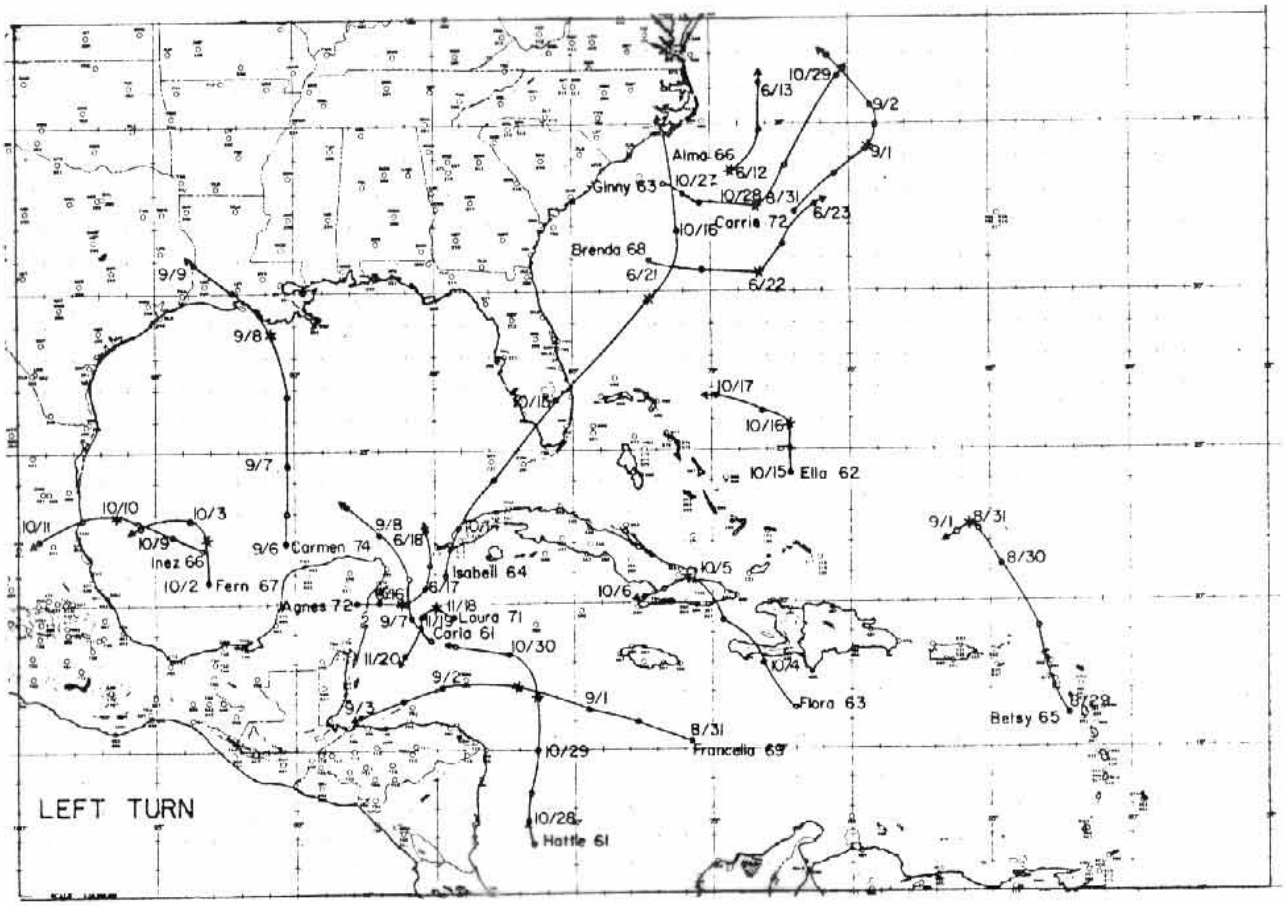

Fig. 12.20. Tracks of 1961-74 Atlantic tropical cyclones with a left-turning motion. The asterisk on each track indicates the turn time T. The solid circle is the 0000 GMT position (with the data next to it) and the open circle is the 1200 GMT position. (After Chan, et al., 1980).

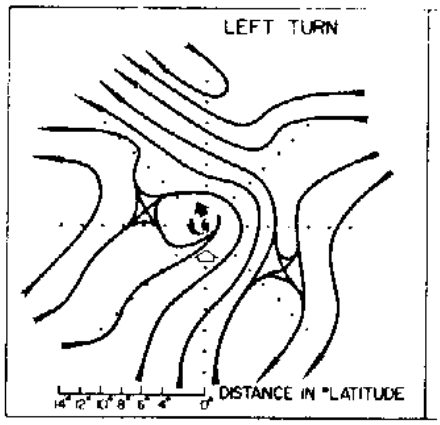

Fig. 12.21. As in Fig. 12.13 except for left-turning tropical cyclones (from Chan et al., 1980).

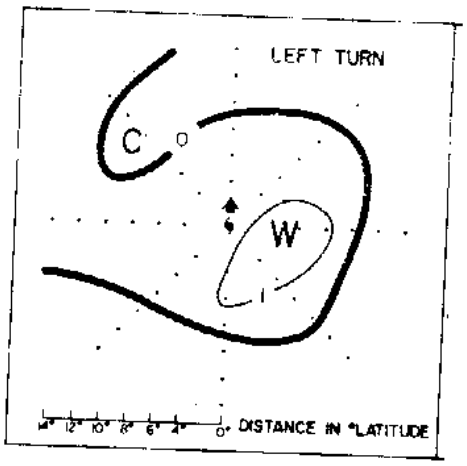

Fig. 12.22. As in Fig. 12.15 except for left-turning tropical cyclones (from Chan et al., 1980).

(tropospheric) cold-low to their west. These two sets of observations therefore appear to be consistent with each other.

These recent studies on left-turning cyclones, together with those on recurvature, all suggest that perhaps the forecasting of a directional change in tropical cyclone motion may be improved if data can be acquired in "critical" regions around the cyclone. Special reconnaissance missions may be flown to provide a better definition of the mid-tropospheric environmental flow, as have been proposed by the U.S. National Hurricane Research Laboratory (American Meteor. Soc., 1981). In regions where such missions are financially impossible, the best hope for improving the prediction of turning motion is through a better use of satellite-derived data such as winds at the upper and lower troposphere as well as mean tropospheric temperatures as proposed by Gray (1979) and Chan et al. (1980). Dvorak (1984) has also suggested the possible use of moisture signatures on satellite pictures to predict tropical cyclone recurvature.

12.5 Binary Cyclones

In a large ocean basin like the northwest Pacific, it is not unusual to have two tropical cyclones present at the same time. An example of this is shown in Fig. 12.23. As the separation between these two cyclones decreases, their circulation may interact with each other, often resulting in rather erratic and thus hard-to-predict tracks for both cyclones. This phenomenon was first discussed by Fujiwhara (1921) and is therefore commonly referred to as the Fujiwhara effect. The forecast errors associated with binary cyclones are in general greater than the average. Brand (1970) found that the average 24h forecast error for 15 binary systems in the northwest Pacific between 1960 and 1967 is 159 n.mi. vs. a mean annual error of 140 n.mi.

Based on laboratory experiments and dynamic arguments, Fujiwhara (1923, 1931) concluded that cyclonic vortices tend to rotate around each other cyclonically. They also have a tendency to attract each other. Haurwitz (1951) used a sample analytic model to explain the rotation of two vortices about each other in terms of the center of mass of the binary system. He found a reasonable agreement between this theoretical result and observations. In cases where disagreement exists, he attributed the discrepancies to the paucity of observations and the possible presence of horizontal and vertical shears in the atmosphere. In an observational study of binary systems, Hoover (1961) found conflicting results in the interaction pattern between cyclones in the northwest Pacific and those in the Atlantic. He suggested the difference in large-scale flow as the main cause for the discrepancies in the results between the two ocean basins.

In a later study, Brand (1970) showed a dependence of the Fujiwhara

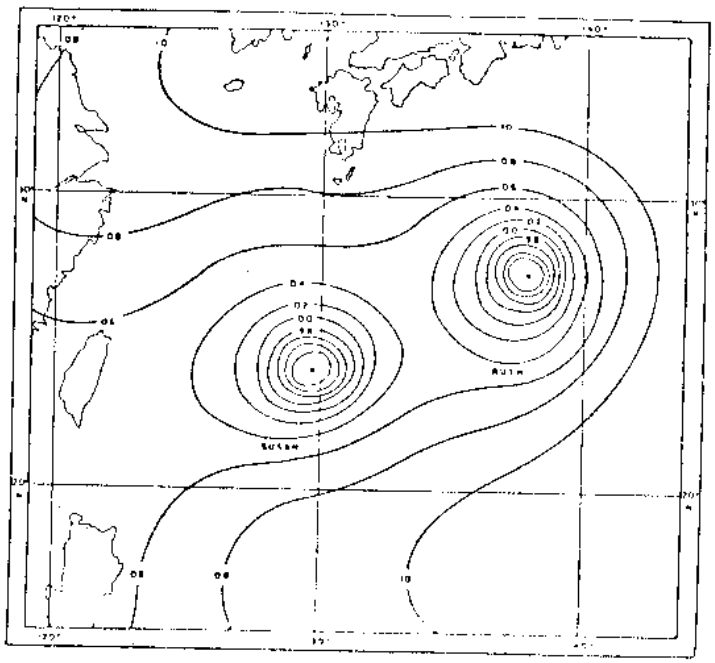

Fig. 12.23. Surface pressure analyses of binary typhoons in the northwest Pacific on 24 August 1945, 0600 GMT (after Haurwitz, 1951).

effect on the separation distance between the two cyclones (Fig. 12.24). It appears that not much rotation takes place when the cyclones are separated by more than 750 n.mi. As the separation distance decreases, the angular change increases in a quadratic manner. In addition, more than half of the binary systems show an attraction towards each other (as shown by a decrease in separation distance with time). This percentage of attracting binary systems increase to 100% when the initial separation distance is less than 400 n.mi. Brand (1970) again emphasized the dependence of the Fujiwhara effect on the large-scale flow.

Dong and Neumann (1983) recently studied northwest Pacific binary cyclones between the years 1949-78 and showed that especially when one of the cyclones is undergoing recurvature as a result of the environmental flow, the binary system can exhibit a clockwise rotation even though the two cyclones might have a separation distance of less than 550 km. However, most of the cyclones that are situated in the Inter-Tropical Convergence Zone (ITCZ) exhibit counterclockwise rotation. The rate of such a rotation again depends on the separation distance. When the two cyclones are less than 650 km apart, the Fujiwhara effect is dominant. On the other hand, if the cyclones are separated further apart, the influence from the flow associated with the ITCZ is greater. Dong and Neumann (1983) therefore concluded that in order to isolate the Fujiwhara effect, the large-scale flow must be filtered.

Since this is difficult to achieve, Chang (1983) tried to simulate the Fujiwhara effect numerically. He found that the model vortices do not exhibit a mutual attraction when the atmosphere is non-divergent.

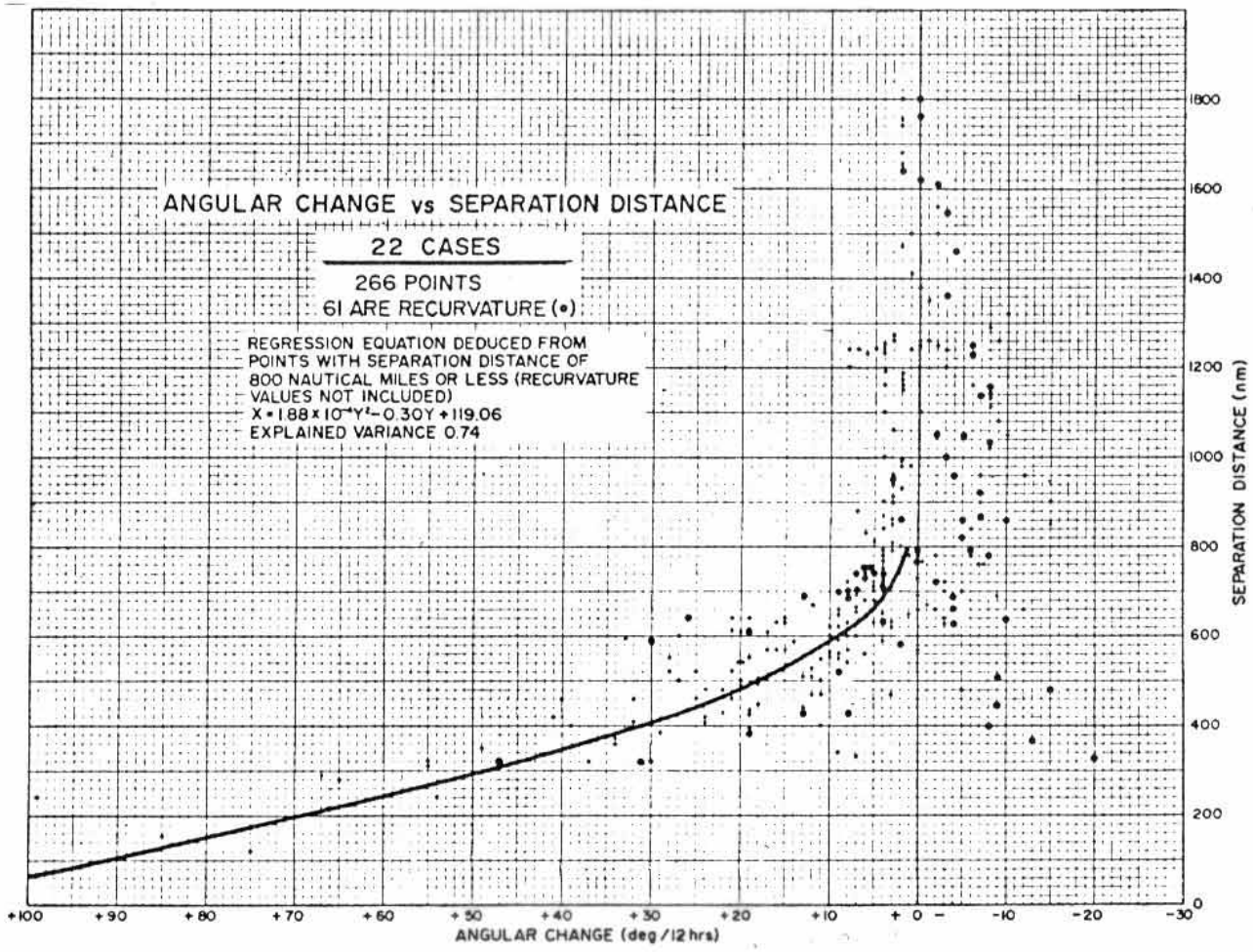

Fig. 12.24. A plot of the 12-hr angular change vs. average separation distance between northwest Pacific tropical cyclone pairs over the 12-hr period (after Brand, 1970).

However, in a three-dimensional model, the vortices rotate around each other and eventually merge to become a single vortex. He, therefore, concluded that advection (of vorticity) alone cannot explain the rotation and mutual attraction of tropical cyclones. Divergence must be included in order to simulate the Fujiwhara effect.

This point of view is questioned by DeMaria and Chan (1984) who were able to simulate the rotation about each other as well as the merging of two vortices in a non-divergent barotropic model atmosphere. The main difference between these two studies is in the size and shape of the vortices. Chang (1983) considered a small vortex with DeMaria and Chan (1984) tested both large and small vortices. The latter authors found that the Fujiwhara effect was only present in the case of large vortices.

Therefore, it appears that although the phenomenon of rotating binary cyclones is very well documented, the physical processes involved in the rotation as well as merging still need to be investigated further. Empirical studies have pointed to some important factors to be considered in estimating the rotation rate and change in separation distance. But until a better physical understanding of the phenomenon can be made, the prediction of the tracks of binary systems will remain a challenging and formidable task.

12.6 Looping

An isolated loop such as that shown in Fig. 12.25 is most frequently caused by changes in the steering flow. However, a loop or a series of loops – as in the trochoidal track in Fig. 12.26 – can also occur as a result of dynamic instabilities.

A typhoon being steered by a strong ridge which suddenly retreats finds itself moving into a col region where there is no balancing pressure gradient. The storm may therefore initially undergo an inertial loop in a clockwise direction (N hemisphere) and then wallow around for several days making loops in either direction as it moves under changing internal forces or is influenced by different environmental flow patterns such as those due to waves in the westerlies passing to the north or easterlies to the south. Tropical storm Susan 1972 made five loops in six days [Fig. 10.7(1)], while under radar observation, before being caught up by a westerly trough. Most periods of looping end by the storm being carried away northward and then northeast because, on average, cyclones tend northward towards the westerlies in the absence of a significant steering current.

A remarkable example of trochoidal motion is shown in the track of typhoon Orchid (1980) in Fig. 12.26. Between 9 September and 11 September the typhoon moved at an average speed of 7 m s^{-1} and executed three cyclonic loops at high speed. During the 10 September the average speed was as high as 9.6 m s^{-1} . The staff at the JTWC Guam, who analyzed this track, believed that loops made by the 700 mb centre were not as large as those made by the surface centre.

The possible physical processes which might explain the trochoidal motion of tropical cyclones have been presented in section 12.3.3. In

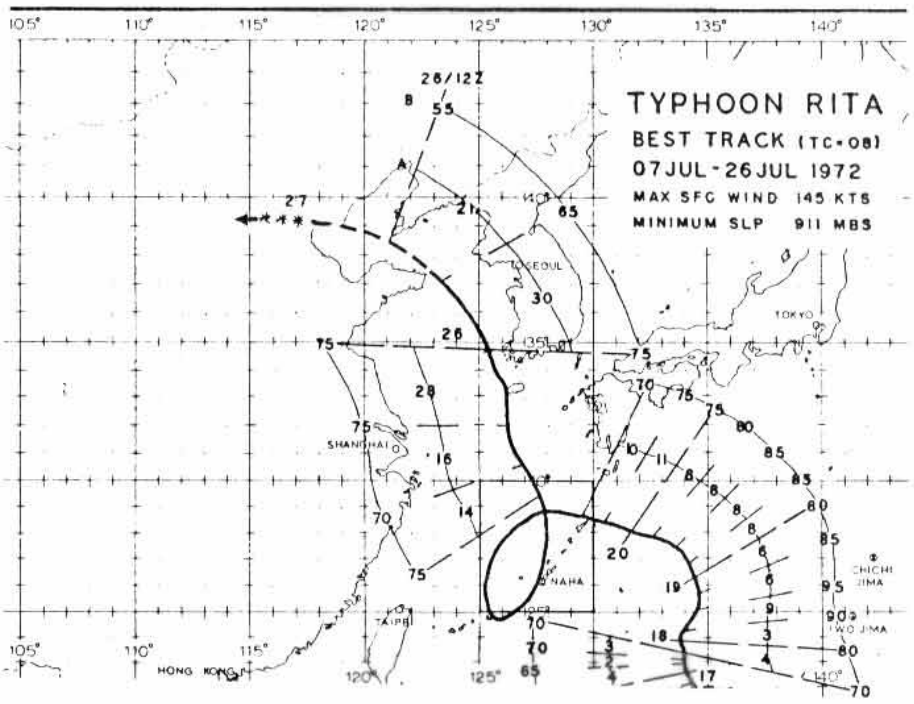

Fig. 12.25. An example of a looping typhoon in the northwest Pacific (adopted from the Annual Typhoon Report 1972, Joint Typhoon Warning Center, Guam).

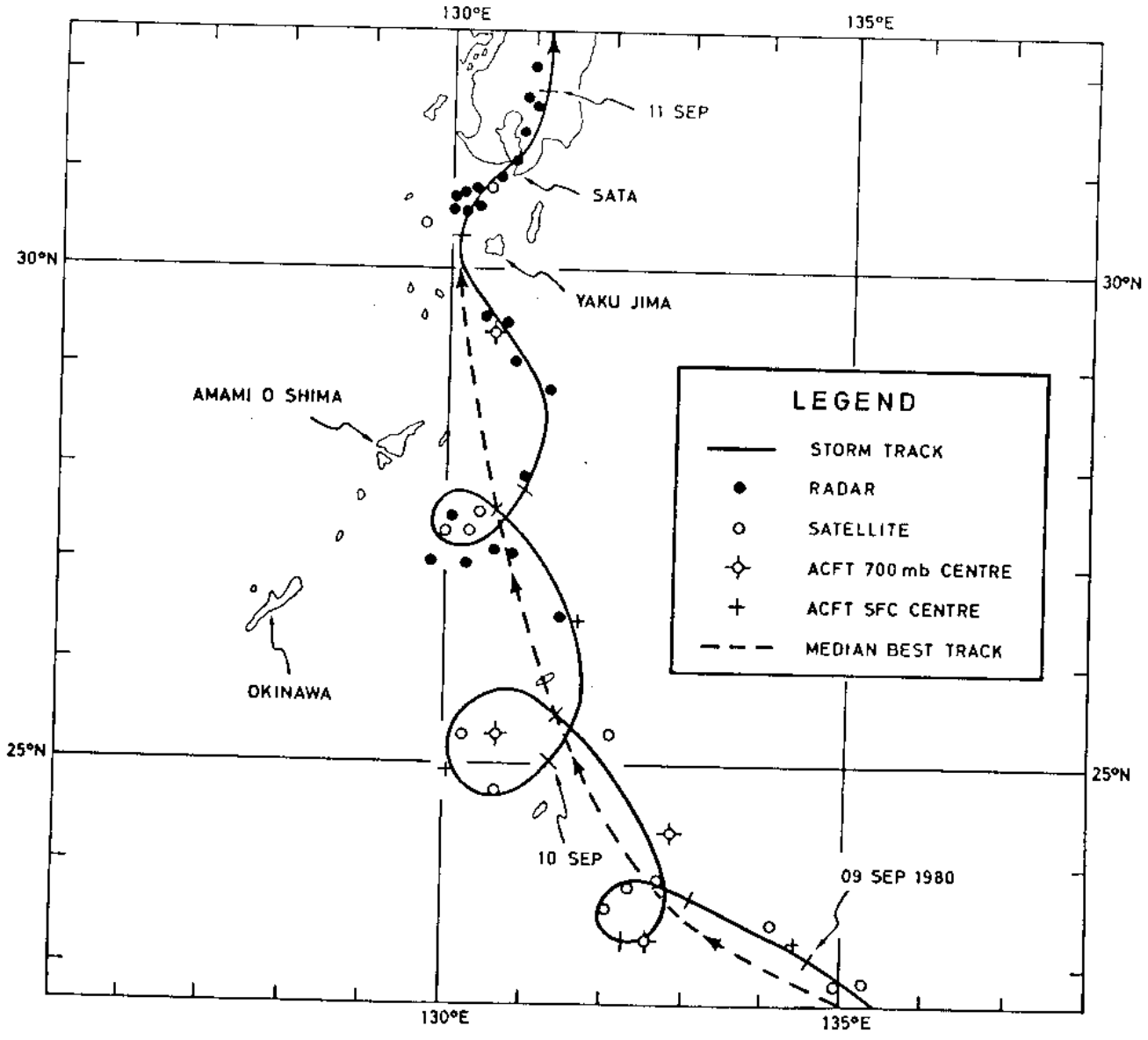

Fig. 12.26. High speed cyclonic loops made by tropical Orchid in the period 9–11 September 1980 (after JTWC Report 1980).

this section, some of the synoptic features associated with the looping motion of the cyclone will be discussed. It must be noted, however, that besides these general characteristics, other conditions might also cause a cyclone to loop. The most common example is when two cyclones are present at the same time. In this case, the cyclonic circulation of one cyclone could cause the other cyclone (situated to its west side) to move southward. As the influence of the first cyclone diminishes, the large-scale circulation could then move the second cyclone northward again, thus forming a loop in its track. The relative motion of binary cyclones has already been discussed in the last section. Here, only the synoptic features associated with a single cyclone will be described.

The most comprehensive study of looping motion has been made by Xu and Gray (1982). They studied 112 looping cyclones in both the northwest Pacific and the west Atlantic between the years 1957-1977. The synoptic flow patterns associated with each case was analyzed. Each cyclone was then classified according to its location into one of the three categories: north of the subtropical ridge at 500 mb, on the ridge, and south of the ridge. The large-scale features for cyclones within each category were found to be very similar, not only among the cases, but also to cyclones that have a translation speed of less that 2.5 m s^{-1}. The surface and 500 mb flow patterns for the three categories are shown in Figs. 12.27-12.29. Notice in all cases, the looping cyclone is situated in a col region at 500 mb, an indication of weak environmental circulation. In addition, a fast-moving short-wave can be identified at this level.

For looping cyclones north of the subtropical ridge (Fig. 12.27), a 500 mb trough is present to the northwest of and at ~ 20^{o}-30^{o} latitude

from the cyclone. Xu and Gray reported that in most cases, this trough is developing and moving. At the surface, a high pressure cell can be seen to the north of the cyclone. The cell therefore provides a steering current that is opposite to that at 500 mb. This phenomenon of opposing flow at different directions is present in almost all cases of slow and looping motion in all three categories. On the other hand, Xu and Gray found that for fast-moving cases (translating speed > 7.5 m s^{-1}), the flows at the surface and 500 mb are parallel to each other. Therefore, as previously discussed, it is very important to identify the steering flow at more than one level in the prediction of cyclone motion.

In Fig. 12.28, a 500 mb trough is seen to the northeast of and at 10^{o}–20^{o} latitude from the looping cyclone situated near the subtropical ridge. Again, a short-wave is moving through the trough. A surface ridge is also present to the north of the cyclone.

A rather different situation is found for looping cyclones present to the south of the 500 mb subtropical ridge (Fig. 12.29). The 500 mb trough is at about the same longitude of but at a large distance ($> 20^{o}$ latitude) from the cyclone. The cyclone is situated in a col region at both the surface and 500 mb.

Two major features appear to be common among the three categories: 1) the passage of a short-wave which modifies the steering flow, and 2) opposing steering flows at the surface and 500 mb. Another important point in trying to anticipate a possible looping of the cyclone is that only should the flow features to the northwest of the cyclone be monitored, the presence of a trough to the north or northeast of the cyclone must also be identified. Since looping cyclones are generally

in a col region, their motion will be dictated by a combination of internal forces and transient synoptic features (such as the passage of a short-wave). Knowledge and understanding of these factors may aid in the predicting of a looping motion.

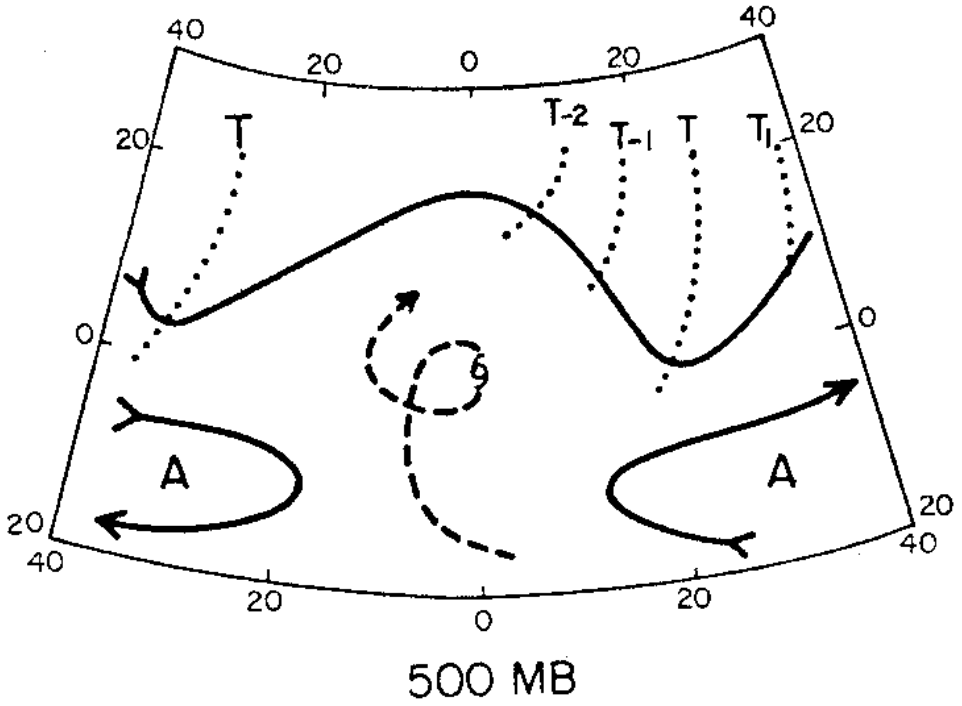

Fig. 12.27(a). Typical flow pattern for slow moving and looping tropical cyclones north of the subtropical ridge. The westerly trough is in 20-30° longitude to the east and north of the cyclone. The dotted lines indicate the trough position at different times, each separated by 12h (from Xu and Gray, 1982).

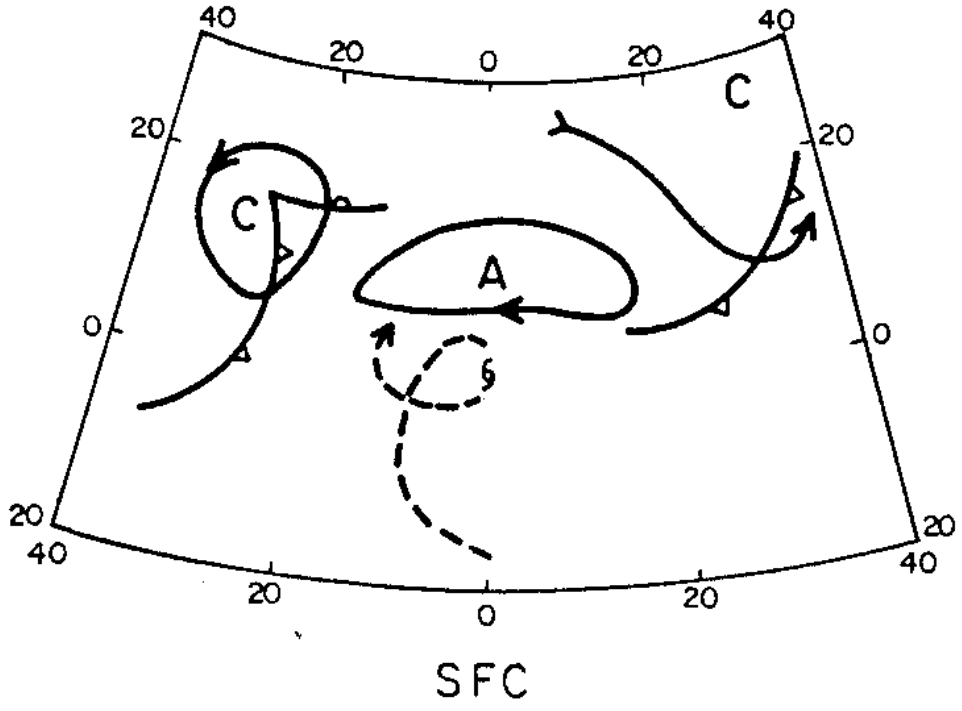

Fig. 12.27(b). Typical surface conditions with Fig. 12.27(a). A surface high pressure cell is located to the north of the cyclone (from Xu and Gray, 1982).

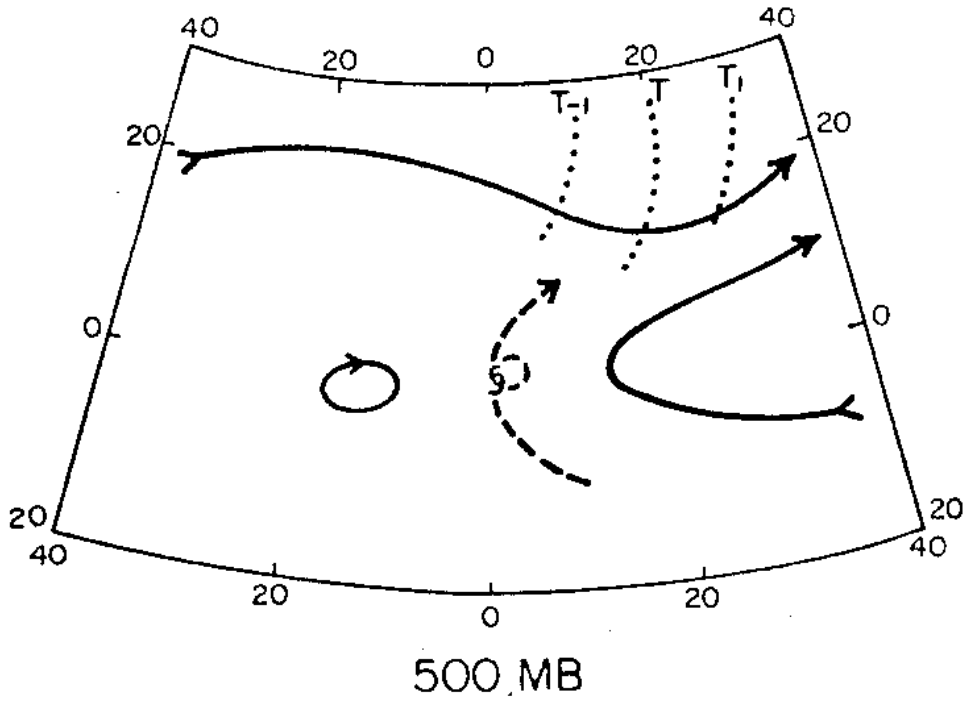

Fig. 12.28(a). As in Fig. 12.27(a) except for slow moving and looping tropical cyclones near the subtropical ridge. A westerly trough is located 10-20° to the northeast of the cyclone (from Xu and Gray, 1982).

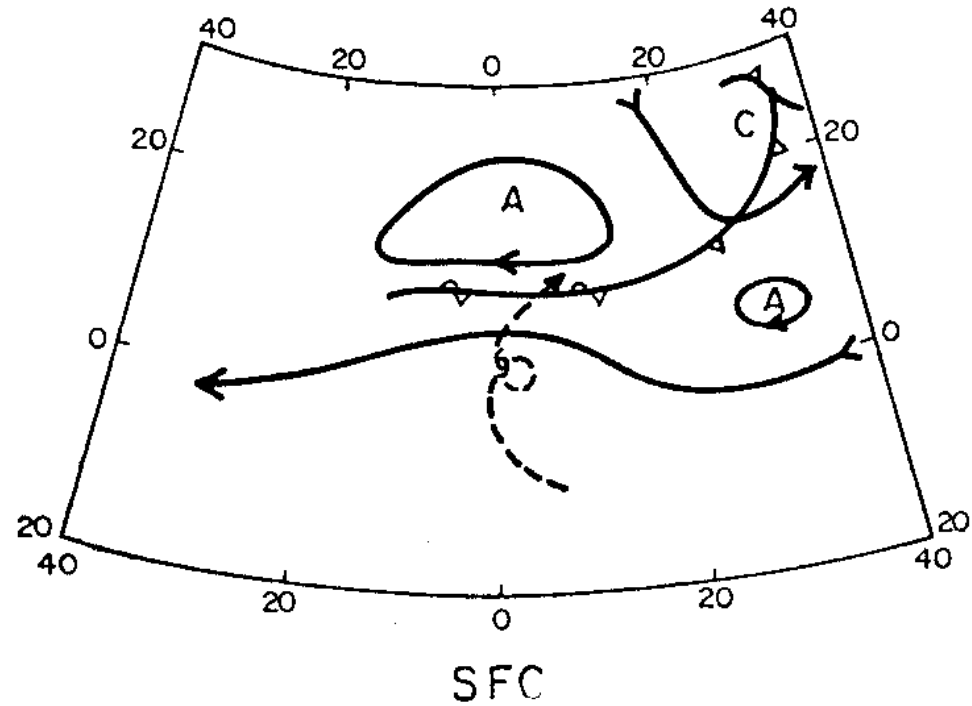

Fig. 12.28(b). Typical surface conditions associated with Fig. 12.28(a). A surface high pressure is to the north of the cyclone (from Xu and Gray, 1982).

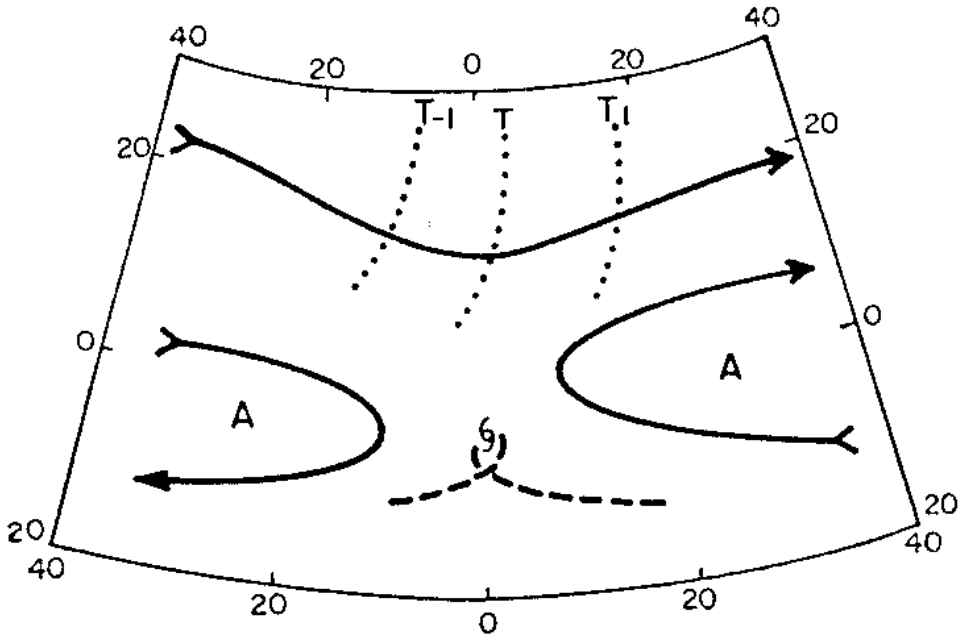

500 MB

Fig. 12.29(a). As in Fig. 12.27(a) except for slow moving and looping tropical cyclones south of the subtropical ridge. A westerly trough is located at about the same longitude to the north (from Xu and Gray 1982).

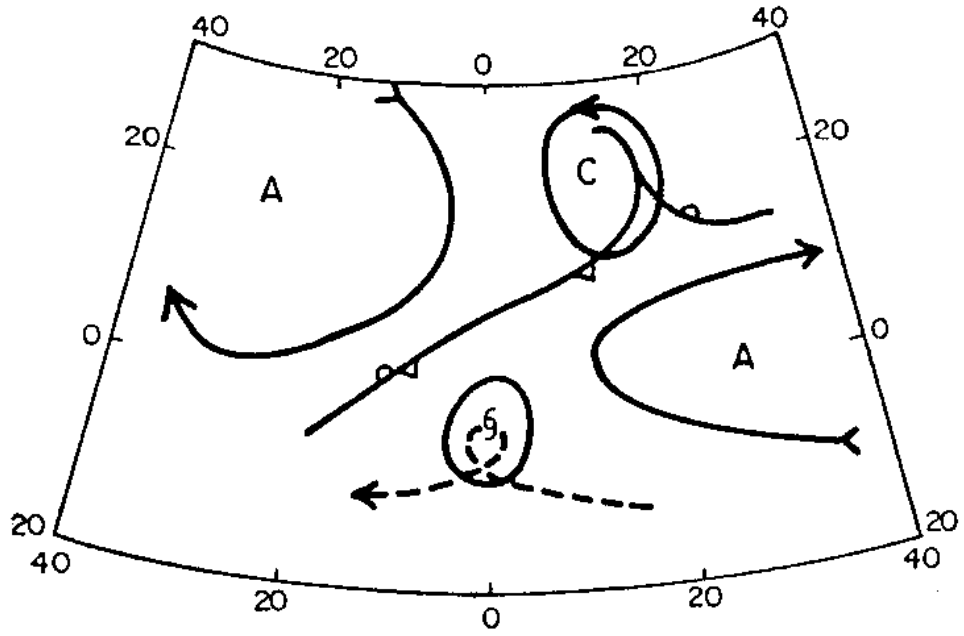

SFC

Fig. 12.29(b). Typical surface map associated with Fig. 12.29(a). The surface cyclone is also located near a neutral point in the flow field (from Xu and Gray, 1982).

12.7 Sea Surface Temperature

So far in this chapter, the factors that might control or modify the path of a tropical cyclone have been discussed mostly in terms of processes in the free atmosphere. In section 12.3.4, the effects of friction on cyclone tracks have also been addressed. Since over most of its lifetime, a cyclone traverses over open water, it seems therefore natural to consider if sea surface temperature (SST) can affect the movement of the cyclone.

It is well-known that the SST must be above a certain threshold (usually taken as 26.5^{o}C) before a tropical cyclone can form and maintain itself (see, e.g. Gray, 1979). Brand (1971) analyzed 14 typhoon pairs in which one typhoon followed the other and found that on the average, the "wake-following" typhoon tended to move away from the path of the first typhoon. He therefore concluded that the cool water due to upwelling caused by the first typhoon deflects the second typhoon. However, Ramage (1974) showed in a case study of three typhoons in the South China Sea that none of the typhoons moved away from the cool water. These conflicting results may be due to the inhomogeneity of the data sample so that other factors may have dictated the movement of the cyclones over the effects of the SST.

Chang and Madala (1980) therefore attempted to study the behavior of model votices subject to different boundary conditions near the surface. This should then simulate the effect of different SSTs (which corresponds to different sensible and latent heat fluxes) on the path of a tropical cyclone. They found that when the SST gradient is normal to the mean flow, the model vortex tends to move towards the warm water side. This result apparently is due to the increase in latent heat flux

which then leads to an increase in convection and hence the movement of the vortex. When the warm SST is to the right of the cyclone, the increased surface convergence due to the stronger winds enhances the evaporation so that a larger deflection from the mean flow results (compared with the case of warm water to the left of the cyclone).

Chang and Madala also studied the cases in which a strip of cold or warm SST is situated parallel to the mean flow and downstream of the cyclone. They found that in either case, the path of the cyclone is not modified. They attributed this result to the fact that the area of warm or cold SST is too small to modify the evaporation significantly. Since in the real atmosphere, the SST is one of the many conditions necessary for monitoring a tropical cyclone, it is not clear to what extent the effect of the SST has on the path of the cyclone. Further numerical experiments that incorporate different atmospheric patterns need to be made to determine such an extent. With the availability of SST values from satellite measurements, observational studies can also be made with greater precision in the selection of cases than in the past.